Expression of NaPi-IIb in rodent and human kidney and upregulation in a model of chronic kidney disease

Motta, Sarah E ; Imenez Silva, Pedro Henrique ; Daryadel, Arezoo ; Haykir, Betül ; Pastor-Arroyo, Eva Maria ; Bettoni, Carla ; Hernando, Nati ; Wagner, Carsten A

Abstract: Na^+-coupled phosphate cotransporters from the SLC34 and SLC20 families of solute carriers mediate transepithelial transport of inorganic phosphate (Pi). NaPi-IIa/Slc34a1, NaPi-IIc/Slc34a3, and Pit-2/Slc20a2 are all expressed at the apical membrane of renal proximal tubules and therefore contribute to renal Pi reabsorption. Unlike NaPi-IIa and NaPi-IIc, which are rather kidney-specific, NaPi-IIb/Slc34a2 is expressed in several epithelial tissues, including the intestine, lung, testis, and mammary glands. Recently, the expression of NaPi-IIb was also reported in kidneys from rats fed on high Pi. Here, we systematically quantified the mRNA expression of SLC34 and SLC20 cotransporters in kidneys from mice, rats, and humans. In all three species, NaPi-IIa mRNA was by far the most abundant renal transcript. Low and comparable mRNA levels of the other four transporters, including NaPi-IIb, were detected in kidneys from rodents and humans. In mice, the renal expression of NaPi-IIa transcripts was restricted to the cortex, whereas NaPi-IIb mRNA was observed in medullary segments. Consistently, NaPi-IIb protein colocalized with uromodulin at the luminal membrane of thick ascending limbs of the loop of Henle segments. The abundance of NaPi-IIb transcripts in kidneys from mice was neither affected by dietary Pi, the absence of renal NaPi-IIc, nor the depletion of intestinal NaPi-IIb. In contrast, it was highly upregulated in a model of oxalate-induced kidney disease where all other SLC34 phosphate transporters were downregulated. Thus, NaPi-IIb may contribute to renal phosphate reabsorption, and its upregulation in kidney disease might promote hyperphosphatemia.

DOI: https://doi.org/10.1007/s00424-020-02370-9

Originally published at:
Motta, Sarah E; Imenez Silva, Pedro Henrique; Daryadel, Arezoo; Haykir, Betül; Pastor-Arroyo, Eva Maria; Bettoni, Carla; Hernando, Nati; Wagner, Carsten A (2020). Expression of NaPi-IIb in rodent and human kidney and upregulation in a model of chronic kidney disease. Pflügers Archiv : European Journal of Physiology, 472(4):449-460.
DOI: https://doi.org/10.1007/s00424-020-02370-9

Expression of NaPi-IIb in rodent and human kidney and upregulation in a model of chronic kidney disease

Sarah E. Motta*, Pedro Henrique Imenez Silva*, Arezoo Daryadel, Betül Haykir, Eva Maria Pastor-Arroyo, Carla Bettoni, Nati Hernando and Carsten A. Wagner

Institute of Physiology, University of Zurich, Switzerland and National Center of Competence in Research NCCR Kidney.CH, Switzerland

*Both authors contributed equally

Corresponding author:
Carsten A. Wagner
Institute of Physiology
University of Zurich
Winterthurerstrasse 190
CH-8057 Zurich
Switzerland
Email: Wagnerca@access.uzh.ch
Phone: +41 44 6355023
ORCID:

Acknowledgments: This study was supported by a grant from the Swiss National Science Foundation to C.A.W (31003A-176125) and the National Center of Competence in Research NCCR Kidney.CH, Switzerland.

Abstract

Na^+-coupled phosphate cotransporters from the SLC34 and SLC20 families of solute carriers mediate transepithelial transport of inorganic phosphate (Pi). NaPi-IIa/Slc34a1, NaPi-IIc/Slc34a3 and Pit-2/Slc20a2 are all expressed at the apical membrane of renal proximal tubules, and therefore contribute to renal Pi reabsorption. Unlike NaPi-IIa and NaPi-IIc, which are rather kidney-specific, NaPi-IIb/Slc34a2 is expressed in several epithelial tissues, including intestine, lung, testis and mammary glands. Recently, the expression of NaPi-IIb was also reported in kidneys from rats fed on high Pi.

Here, we systematically quantified the mRNA expression of SLC34 and SLC20 cotransporters in kidneys from mice, rats and humans. In all three species, NaPi-IIa mRNA was by far the most abundant renal transcript. Low and comparable mRNA levels of the other four transporters, including NaPi-IIb, were detected in kidneys from rodents and humans. In mice, the renal expression of NaPi-IIa transcripts was restricted to the cortex whereas NaPi-IIb mRNA was observed in medullary segments. Consistently, NaPi-IIb protein colocalized with uromodulin at the luminal membrane of thick ascending limbs of the loop of Henle segments. The abundance of NaPi-IIb transcripts in kidneys from mice was neither affected by dietary Pi, the absence of renal NaPi-IIc, nor the depletion of intestinal NaPi-IIb. . In contrast, it was highly upregulated in a model of oxalate-induced kidney disease where all other SLC34 phosphate transporters were downregulated. Thus, NaPi-IIb may contribute to renal phosphate reabsorption and its upregulation in kidney disease might promote hyperphosphatemia.

Keywords (5-6)

Phosphate, Slc20, Slc34, kidney, epithelia transport

Introduction

Transport of inorganic phosphate (Pi) across the apical membrane of mammalian epithelial cells is mediated by Na^+-coupled Pi cotransporters from the Slc34 and Slc20 families of solute carriers (for review see [21,5,72]). Both families use the electrochemical gradient of Na^+ as driving force for the uphill transport of Pi, but whereas Slc34 proteins couple the uptake of one divalent Pi to the transport of either 2 or 3 Na^+ ions, the Slc20 orthologues transport one monovalent Pi together with 2 Na^+ ions [20]. The three members of the Slc34 family (Slc34a1/NaPi-IIa, Slc34a2/NaPi-IIb and Slc34a3/NaPi-IIc) have an overall peptide identity of about 50% that increases to roughly 80% in the predicted transmembrane domains. The two Slc20 proteins (Slc20a1/Pit-1 and Slc20a2/Pit-2) are also highly conserved (overall identity of 60%). However, the homology between Slc34 and Slc20 members is no higher than 10%.

Renal reabsorption of Pi takes place along the proximal tubules, with early studies providing contradictory data regarding a potential contribution of distal parts of the nephron [1,67,11,39,31,24]. NaPi-IIa, NaPi-IIc and Pit-2 are expressed at the brush border membrane (BBM) of proximal tubular cells, and their abundance is regulated by several hormones, including parathyroid hormone (PTH), fibroblast growth factor 23 (FGF23) and dopamine, as well as by dietary Pi. Low dietary Pi upregulates the expression of the three renal cotransporters, which consequently increases Pi reabsorption and reduces urinary excretion of Pi [42,71,10]. Instead high dietary Pi [71,10,42], PTH [53,36,52,65,16,18], FGF-23 [63,66,14,38,70] and dopamine [2,16] reduce their expression and, therefore, have a phosphaturic effect. In mice, ablation of NaPi-IIa results in hypophosphatemia due to urinary loss of Pi, despite a two-fold increase in NaPi-IIc abundance [3]. In contrast, the absence of NaPi-IIc does not disturb Pi homeostasis [64,48]. However, mutations in both SLC34A1/NaPi-IIa [55,60,19] and SLC34A3/NaPi-IIc [4,29,41] have been identified in patients with renal loss of phosphate and hypophosphatemia demonstrating that both transporters are critical in humans (for review see [73,40]).

Intestinal absorption of Pi is proposed to involve both passive/paracellular and active/transcellular mechanisms. NaPi-IIb, Pit-1 and Pit-2 are expressed among other tissues in intestinal epithelia (for review see [27]), though whether or not they are the only active intestinal transporters remains an open issue [12]. The relative abundance of NaPi-IIb along the different intestinal segments seems to be species-specific. In mice, this transporter is mostly found in the ileum [54], whereas in rats [22,44] it is preferentially expressed in duodenum and jejunum. A higher contribution to intestinal Pi absorption of jejunum than ileum was also suggested in humans [33,74]. Studies in Slc34a2 knockout mice indicate that NaPi-IIb is responsible for more than 90% of the active Pi absorption by the small intestine though its overall contribution to intestinal absorption is not bigger than 50% [26,58]. The

pattern of expression of Pit transporters along the gut is also different in rats [22,12] and mice (Pastor-Arroyo, unpublished data). Dietary Pi also controls the abundance of intestinal cotransporters, with high and low dietary Pi inducing their downregulation and upregulation, respectively [13,22,25,62,54,34]. The expression of NaPi-IIb in the intestinal epithelia is stimulated by 1,25 $(OH)_2$ vitamin D_3 [25,76,45].

In addition to kidney and/or intestine, Pit-1, Pit-2 and NaPi-IIb are widely expressed. High levels of Pit-2 are found in the brain [30], where the transporter may be involved in controlling Pi in the cerebrospinal fluid. Mutations in Pit-2 are one of the causes of familial idiopathic basal ganglia calcification (FIBGC) [75], a disease recapitulated in Pit-2 deficient mice [32]. Both Slc20 transporters were recently proposed to contribute to extracellular Pi sensing [7,8]. Expression of NaPi-IIb mRNA has been reported in several organs including lungs, mammary glands, liver and testis [28]. Although very little is known about its role in these tissues, mutations in NaPi-IIb cause pulmonary alveolar microlithiasis (PAM) and may as well associate with testicular microlithiasis [15,59,69]. Indeed, the concentration of Pi in the bronchoalveolar fluid is markedly elevated in NaPi-IIb$^{-/-}$ mice [59]. Expression of NaPi-IIb mRNA was also reportedin kidneys of rats fed high Pi [68]. This study reported the expected reduction of NaPi-IIa and NaPi-IIc abundance in kidneys upon high dietary Pi, whereas the renal mRNA expression of NaPi-IIb was increased in the high Pi fed animals. Surprisingly, a basolateral localization of NaPi-IIb in unidentified nephron segments was reported using an antibody not well validated.

The aims of this work were to compare the expression of NaPi-IIb/SLC34A2 to the other members of the SLC34 and SLC20 families in kidneys from mice, rats and humans, to identify the tubular segments expressing NaPi-IIb and to investigate potential physiological/pathophysiological conditions able to regulate its renal expression. For the last aim, the abundance of NaPi-IIb transcripts was compared in samples from wild type (WT) mice and in several models deficient for particular Slc34 cotransporters, as well as in WT mice fed with different dietary Pi content or subjected to oxalate-induced renal disease.

Material and Methods

Animals All experiments described below were approved by the local veterinary authority (Kantonales Veterinäramt Zürich) and complied with Swiss Animal Welfare laws.

Mice Experiments were performed with 10-14 weeks WT male mice (C57BL/6J, Janvier, France) as well as with mice with constitutive and global depletion of NaPi-IIa (NaPi-IIa $^{-/-}$) [3], intestinal-specific depletion of NaPi-IIb (NaPi-IIb$^{-/-}$) [26] and renal specific and inducible depletion of NaPi-IIc (NaPi-IIc$^{-/-}$) [48]. For NaPi-IIa$^{-/-}$ and NaPi-IIb$^{-/-}$, WT littermates were used as control, whereas the values of NaPi-IIc$^{-/-}$ (floxed/floxed animals drinking doxycycline) were compared with floxed/floxed mice drinking sucrose. For collection of blood and/or organs mice were anesthetized with 2% isoflurane; samples were snap frozen until further use.

Comparison between genotypes. All animals were fed standard chow (KLIBA: 0.8% Pi, 1% Ca^{2+} and 1000 IU/kg vitamin D_3), and each group consisted of 5 mice.

Dietary adaptation in WT mice. Mice were fed either a standard diet (KLIBA: as above) or diets with low (KLIBA: 0.1% Pi, 1% Ca^{2+} and 1000 IU/kg vitamin D_3) or high (KLIBA: 1.2% Pi, 1% Ca^{2+} and 1000 IU/kg vitamin D_3) Pi content. High and low Pi diets were administered both acutely (18 and 24 hours) and chronically (3 and 5 days). Each dietary group consisted of 5 mice.

Oxalate treatment of WT mice. Mice (male, 12 weeks old) were first adapted for 3 days to a low Ca^{2+}-containing chow (Ssniff: 0.4 Pi and 2200 IU/kg vitamin D_3, no Ca^{2+} added) followed by 4 days administration of a low Ca^{2+} high oxalate diet (Ssniff: 0.4 Pi and 2200 IU/kg vitamin D_3 and 6.7 g sodium oxalate/kg, no Ca^{2+} added), or 4 days low Ca^{2+}-containing chow as a control group. Then, they were left to recover for 4 days on standard chow (KLIBA). On the last day, mice were placed in metabolic cages for collection of 24 hours urine. Blood and kidneys were collected under anesthesia. Each dietary group consisted of 6 mice.

Rats Male Wistar rats were purchased from Charles River (Germany). Experiments were performed on 6 to 8 weeks old rats fed standard diet. For collection of kidneys and intestines, rats were anesthetized with 3% isoflurane; samples were snap frozen until further use.

Human kidneys Non-transplantable human kidneys were obtained from the International Institute for Advancement of Medicine (IIAM; Edison-NJ. USA), with the approval of the local ethics committee. Samples were derived from 2 female and 3 male donors, with an age between 50 and 63 years. Their blood urea nitrogen values ranged between 16 to 39 mg/dL (mean ± SEM: 29.4 ± 5) and their plasma creatinine between 0.73 and 3.1 mg/dL (1.57 ± 0.4). Cortical pieces were processed for RNA isolation.

RNA isolation and semi-quantitative Real-Time PCR (qPCR) RNA was isolated from kidney and intestinal samples using the Qiagen RNeasy Mini extraction kit (Qiagen, Germany). Isolation was done according to the instructions provided by the manufacturer. Purified RNA was then transcribed to cDNA (TaqMan Reverse Transcription Kit, Applied Biosystems) which was later used as template for the PCR. The relative expression of the genes of interest was quantified by using sequence-specific forward and reverse primers together with sequence-specific probes labeled with reporter (5'-end, FAM), and quencher (3'-end, TAMRA) dyes. Custom-designed primers and probes were synthetized by Microsynth (Balgach, Switzerland) whereas commercially-available sets were purchased from Applied Biosystems (supplementary table 1). Hypoxanthine-guanine phospho-ribosyltransferase (HPRT) or 18S were used as housekeeping genes, and their probes were labeled with VIC as reporter dye. qPCR was performed using the 7500 Fast Real Time PCR System, and the obtained data was analyzed with the 7500 Fast Real-Time PCR System Sequence Detection Software v1.4. Ct values were calculated after adjusting the baseline threshold to 0.06. The relative fold change was calculated according to the formula $2^{(Ct\ (control)\ -\ Ct\ (experiment))}$.

***In Situ* Hydridization** Mice were anesthetized with isoflurane, pre-perfused with heparin and perfused with fixative (3% PFA in 0.1 M Na-cacodylate) through the left cardiac ventricle. Kidneys were harvested and processed for embedding (O.C.T. embedding matrix, Cell Path) as previously reported [53]. Embedded and frozen kidneys were stored at -80 °C until further use. Renal sections (5 µm thick) were prepared with a cryotome (Leica Biosystems), and immediately mounted on slides (Superfrost Plus, Thermo Scientific). Renal sections were processed for *in situ* hybridization using the RNAscope 2.5HD Duplex assay as well as the RNAscope 2.5 chromogenic assay (both from Bio-techne) following the manufacturer's recommendations. Briefly, samples were first rehydrated in PBS and then boiled for 5 minutes in a target retrieval solution provided by the kit. Afterward, tissue samples were hybridized for 2 hours at 40°C with NaPi-IIa/*Slc34a1* and/or NaPi-IIb/*Slc34a2* mRNA probes, subjected to signal amplification and incubated with fluorescent or alkaline phosphatase-labelled probes. For the chromogenic assay, samples were then incubated for 10 min at room temperature with Fast Red substrate and counterstaining with Gill's Hematoxylin I. All samples were finally mounted with VectaMount Mounting Medium HT-5000 (Vector Laboratories, Burlingame, CA, USA). Signals were analyzed with a microscope (Leica DM 55008). As negative and positive controls, additional tissue samples were processed in parallel with probes for the bacterial dihydrodipicolinate reductase (*DapB*) and the mouse peptidyl-prolyl cis-trans isomerase B (*Ppib*), respectively.

Western Blot Renal and intestinal BBM were prepared according to the Mg^{2+} precipitation technique [6]. BBM were resuspended in 300 mM Mannitol, 20 mM Hepes-Tris, pH 7.4 and stored at -20 °C. Proteins (25-50 µg of BBM or 75 µg of homogenates) were separated by electrophoresis in 10% SDS-polyacrylamide gels and transferred to PVDF membranes. Membranes were incubated overnight at

4 °C with NaPi-IIb [28] primary antibody (dilution 1: 3,000) followed by 2 hours incubation at room temperature with secondary antibody (anti-rabbit HRP-conjugated IgG diluted 1: 5,000). For the detection of actin, a monoclonal antibody raised in mouse was applied (SIGMA Aldrich, dilution 1: 5,000), using as secondary antibody anti-mouse HRP-conjugated IgG (dilution 1: 10,000). Primary and secondary antibodies were diluted in TBS containing 5% powder milk. All secondary antibodies were purchase from GE Healthcare. After addition of chemiluminescent HRP substrate (Millipore; CDP-star, Roche), chemiluminescence was detected with a LAS-4000 Fujifilm image analyzer. For peptide protection, the antigenic peptide used to raise the NaPi-IIb antibody [28] was incubated for 2 hours at room temperature with the NaPi-IIb antisera (75-100 µg peptide/ml diluted antibody) prior to addition of the antisera to the PVDF membrane.

Immunofluorescence Mouse renal sections (5 µm thick) prepared as indicated above were first subjected to antigen retrieval. For that, samples were microwaved for 5 minutes in 10 mM citrate buffer at pH 6.0, followed by incubation in 1% SDS/PBS for 5 minutes at room temperature. After three washes in PBS, non-specific protein binding was prevented by treatment with blocking solution (1% BSA/PBS) for 15 minutes at room temperature. Cryosections were then incubated overnight in a humidified chamber at 4°C with the following primary antibodies diluted in PBS: sheep anti-Uromodulin (1: 500, Thermo Fisher Scientific, PA5-47706), rabbit anti-NaPi-IIa (1: 2,000 [17]), rabbit anti-NaPi-IIb (1: 1,000 [28]), or rabbit anti-NaPi-IIc (1: 500 [50]). Upon removal of primary antibodies, sections were rinsed three times with PBS and once with hypertonic PBS (18 g NaCl/l PBS) and then incubated for 1 hour at room temperature in the dark with the appropriate secondary antibodies: donkey anti-rabbit Alexa Fluor-594 (1: 500; Life Technologies, A21207) and donkey anti-sheep DyLight-488 (1: 500; Abcam, ab96939). Nuclei were stained by addition of 4', 6-diamidino-2-phenylindole dihydrochloride (DAPI) (1: 500, Sigma, D9542) to the secondary antibody solution. Thereafter, slides were washed twice with hypertonic PBS and once with PBS before being covered with mounting medium (Dako, USA) and coverslips. Slides were viewed using a Leica DM 5500B fluorescence microscope and processed using Adobe Photoshop (Adobe Photoshop, San Jose, CA). Sections of mouse ileum were also subjected to 1% SDS antigen retrieval; then samples were incubated with the NaPi-IIb antibody (1:200) together with DAPI (1:1,000) and phalloidin texas red (1:100). For peptide protection, the NaPi-IIb antibody was pre-incubated with antigenic peptide (100 µg peptide/ml diluted antibody) as indicated above.

Determination of urinary and plasma metabolites Urinary and/or plasma levels of creatinine, urea and Pi were measured with a UniCel DxC 800 Synchron Clinical System in the Zurich Integrative Rodent Physiology (ZIRP) facility. Plasma levels of intact FGF23 were quantify using an Elisa kit (Immunotopics).

Presentation and statistical analysis Data are presented as mean ± SEM. Statistical significance was determined by ANOVA or t-test and $P < 0.05$ was considered as significant.

Results

NaPi-IIa is the Na/Pi cotransporter with higher renal mRNA expression in mice, rats and humans

The mRNA expression of the three members of the Slc34 family of Na/Pi-cotransporters (NaPi-IIa, NaPi-IIb and NaPi-IIc) together with the two members of the Slc20 family (PiTt-1 and Pit-2) was analyzed by qPCR in kidneys of mice and rats and human. To verify that the sets of primers/probe used to quantify each of the five transcripts did actually have similar amplification efficiencies, PCRs were performed using as template progressive cDNA dilutions. Then, a standard curve was constructed by plotting the Ct values against the cDNA concentrations. The efficiency of each set of primers/probe was calculated from the formula $10^{(-1/slope)}$, with a maximal efficiency having a value of 2. As shown in supplementary table 1, for all three species, the amplification efficiency of the five cotransporters mRNAs was found to be very similar, and close to the maximal value. Based on these data, the comparison of different mRNAs abundances is indeed feasible.

In kidneys from mice (Fig. 1A) and rats (Fig. 1B), NaPi-IIa showed by far the highest level of mRNA expression. Although transcripts of all the other cotransporters were also detected, their abundance was about two orders of magnitude smaller than the values detected for NaPi-IIa. Moreover, no major differences were found for the renal mRNA expression of these four cotransporters. Similar to both murine models, cortical preparations from human kidneys express much higher levels of NaPi-IIa mRNA than of the other four genes (Fig. 1C). Interestingly, in the three analyzed species the relative expression of NaPi-IIb mRNA was comparable to the abundance of NaPi-IIc transcripts.

NaPi-IIa and NaPi-IIb are expressed in different and distinct nephron segments in mouse kidney

The pattern of expression of NaPi-IIa and NaPi-IIb transcripts in murine kidneys was next compared by *in situ* hybridization (RNAscope) (Fig. 2A). Analysis of renal slices incubated simultaneously with fluorescent probes for NaPi-IIa (red) and NaPi-IIb (green) indicated that NaPi-IIa mRNA is highly abundant in a cortical population of tubules morphologically identified as proximal tubules, whereas no signal was detected in the medulla. Although far less abundant than NaPi-IIa, a clear signal was also observed with the NaPi-IIb probe (Fig. 2A), confirming the expression of this transporter mRNA in kidney. Tubules positive for NaPi-IIb mRNA were mostly located in the outer medulla, such that no overlapping of both cotransporters was observed. Expression of NaPi-IIb transcripts in medullary segments was further confirmed using a chromogenic *in situ* hybridization probe: as shown in Fig. 2B, the NaPi-IIb chromogenic probe provided a stronger signal than the fluorescence probe. No signal was

observed in sections incubated with a probe for the bacterial dihydrodipicolinate reductase (data not shown). The segments expressing NaPi-IIb mRNA were likely thick ascending limbs (TAL) of the loop of Henle. This was further supported by the analysis of published data from two different databases reporting single cell transcriptome data from mouse kidney [51,56] (see supplementary figure 4). Data from Park *et al*. showed high abundance of NaPi-IIa mRNA in all nephron segments with a strong peak in proximal tubule. NaPi-IIc mRNA was also localized to proximal tubule, whereas NaPi-IIb transcripts were mostly found in TAL of the loop of Henle [51]. A more detailed analysis of the male and female murine kidney reported by Ransick *et al*, demonstrates selective expression of NaPi-IIa and NaPi-IIc mRNA in the proximal tubule of both male and female kidneys. In both genders, NaPi-IIb mRNA is restricted to the thin descending and ascending limbs of the loop of Henle as well as the TAL [56].

The renal presence of NaPi-IIb at the protein level was then analyzed by immunofluorescence and its pattern of expression compared with that of NaPi-IIa and NaPi-IIc. As expected, the expression of NaPi-IIa and NaPi-IIc was restricted to the BBM of renal proximal tubules (Fig. 3A, C), and none of them colocalized with uromodulin. In agreement with the *in situ* hybridization data, incubation with a NaPi-IIb antibody labeled the luminal side of a small population of medullary tubules, mostly located in the outer medulla, that were also positive for uromodulin (Fig. 3B). The specificity of the NaPi-IIb antibody was demonstrated by peptide protection of immunostainings of ileum sections as well as of Westernblot of ileum homogenates (supplementary Fig. 1): in both cases the NaPi-IIb-related signal was abrogated upon preincubation of the antibody with the immunogenic peptide consistent with the absence of signal in intestine-specific NaPi-IIb KO mice using the same antibody [26]. Although Westernblots detected a faint band at the expected size in protein samples from mouse kidney, this signal is most probably unspecific, as its intensity was not reduced upon peptide protection (supplementary Fig. 1E, F). Furthermore, no band corresponding to NaPi-IIb was detected in kidneys from mice fed acutely (1 day) or chronically (5 days) with high or low Pi diets (data not shown).

NaPi-IIb is the Na/Pi cotransporter with higher mRNA expression in mouse ileum and rat jejunum

The expression of Slc34 and Slc20 cotransporters was also compared in intestinal segments, namely ileum from mice and duodenum and jejunum from rats (supplementary Fig. 2). These segments were selected based on available data showing that in mice active intestinal transport of Pi proceeds mostly along the ileum [54], whereas duodenum and jejunum are the segments responsible for active intestinal absorption in rats [22,44]. In ileum from mice, the expression of NaPi-IIb mRNA was between 3 orders (vs. Pi1-1 and Pit-2) to 4 orders (vs. NaPi-IIa and NaPi-IIc) of magnitude higher than the expression of the other cotransporters (supplementary Fig. 2A), consistent with the major role of NaPi-IIb in active intestinal absorption of Pi suggested in recent publications [26,58]. Also in rat duodenum, the expression of NaPi-IIb transcripts was far higher than that of other transporters (supplementary

Fig. 2B). Instead, similar expression of NaPi-IIb and Pit-1 mRNAs was detected in rat jejunum (supplementary Fig. 2C), whereas the expression of the other cotransporters was between one order (vs. Pit-2) to 3 orders (vs. NaPi-IIa and NaPi-IIc) of magnitude lower.

Renal expression of Na/Pi cotransporters mRNAs in mice is not altered by dietary phosphate or by the absence of Slc34 paralogues

The renal abundance of Slc34 and Slc20 transcripts was compared in kidney samples from wild type mice fed acutely (18 and 24 hours) and chronically (3 and 5 days) with diets containing either low (0.1%) or high (1.2%) Pi. As shown in Fig 4, the expression of the analyzed cotransporters was altered neither after 18 hours (A) nor after 5 days (B), except for small changes in Pit-2 and NaPi-IIc expression in the acute and chronic diets, respectively. Comparable mRNA levels were also found in samples from mice fed 24 hours or 3 days with either high or low Pi diets, except for a small downregulation of NaPi-IIc expression in mice fed 3 days on high Pi (data not shown).

The renal mRNA expression of all Slc34 and Slc20 cotransporters was also compared in mouse models deficient for Slc34 members either in kidney (NaPi-IIa and NaPi-IIc) or in intestine (NaPi-IIb). Neither the absence of renal NaPi-IIa (Fig. 5A) or renal NaPi-IIc (Fig. 5C) not depletion of intestinal NaPi-IIb (Fig. 5B) resulted in major changes in the renal expression of the remaining cotransporters, with only a small upregulation of NaPi-IIb expression in NaPi-IIa deficient mice.

Renal expression of Na/Pi cotransporters mRNAs is differentially altered in mice with oxalate-induced nephropathy

Feeding mice for 4 days with a high oxalate diet resulted in elevated plasma levels of creatinine and urea (supplementary Fig. 3) as well as in reduced creatinine clearance (Fig. 6A) as reported earlier for this model of oxalate nephropathy [46]. Furthermore, urinary excretion of Pi tended to be reduced (Fig. 6B) whereas plasma Pi was increased (Fig. 6C). The circulating concentration of intact FGF-23 (Fig. 6D), as well as the renal mRNA levels of *Ffg23* (Fig. 6E) and tumor necrosis factor (*Tnf*) (Fig. 6F) were all higher in oxalate-treated mice.

Oxalate treatment decreased the renal expression of NaPi-IIa and NaPi-IIc transcripts whereas it resulted in the upregulation of NaPi-IIb mRNA, with little or no effect on both Slc20 transcripts (Fig. 6G).

Discussion

The Slc34 and Slc20 families of Na^+/Pi cotransporters mediate the first step of transcellular transport of Pi across the apical membrane of epithelial cells. NaPi-IIa/Slc34a1 and NaPi-IIc/Slc34a3 are considered to be the major Na^+/Pi cotransporters responsible for the reabsorption of filtered Pi from the primary urine. Here, we report that NaPi-IIa shows by far the highest level of mRNA expression in kidneys from adult mice, rats and humans. This finding is in agreement with the major and unreplaceable role of the cotransporter in mice [3] as well as with its implication in the development of idiopathic infantile hypercalcemia (OMIM **#**616963) in humans (for review see [73]). In contrast, the expression of NaPi-IIc transcripts in all three species was one (rats) to two (mice, humans) orders of magnitude lower than those detected for NaPi-IIa. The relative low expression of NaPi-IIc mRNA in both murine models is in accordance with current literature. Its low expression in adult rats was suggested by antisense hybrid depletion experiments in which depletion of NaPi-IIc mRNA from renal poly(A)$^+$ RNA extracted from young rats was shown to reduce the capacity of the RNA pool to induce Pi-transport in oocytes, whereas depletion from adult samples had no effect [61]. On the other hand, NaPi-IIc ablated mice have an unperturbed Pi homeostasis, suggesting a minor contribution to renal Pi handing in mice [26,64]. Based on the above observations, it is currently accepted that in rodents NaPi-IIc is a juvenile transporter and that its contribution to Pi balance in adults is negligible [61]. However, its low expression level in kidneys from adult humans was unexpected, since it is well established that mutations in NaPi-IIc in humans cause hereditary hypophosphatemic rickets with hypercalciuria, with persistent symptoms in adult patients (HHRH; OMIM **#**241530) (for review see [73]). This apparent discrepancy could be either related to the specific pathological state of the donors, to a lack of correlation between RNA and protein levels, or to a decline on the expression of the cotransporter with age in humans, in a similar way to mice. Interestingly, we could detect renal expression of NaPi-IIb transcripts in all three species analyzed; furthermore, in all cases its abundance was comparable to the levels of NaPi-IIc (and Slc20) mRNAs. Relatively small but consistent mRNA expression of NaPi-IIb in mouse and human kidneys was already reported by Hilfiker *et al* and Nishimura and Naito, respectively [28,49].

As expected, we found that NaPi-IIa mRNA is highly abundant in the cortex and absent from medulla. The cortical expression of NaPi-IIa is in agreement with early reports in which using different techniques (*in situ* hybridization with radioactive probes, and qPCR on RNA extracted from isolated nephron segments) the expression of NaPi-IIa transcripts was shown to be restricted to proximal tubules [43,57]. In a recently published transcriptome study Ransick *et al.* reported single-cell RNA sequencing of adult male and female mouse kidneys [56] (supplementary Fig. 4A). For the analysis, cortical and juxtamedullary nephrons as well as ureteric epithelium were subdivided in up to 32 anatomically and functionally distinct regions, from podocytes to deep medullary epithelium of pelvis

(for details see legend to supplementary Fig. 4). As expected, this study confirmed the presence of NaPi-IIa mRNA specifically in the S1 and S2 segments of proximal tubules of both cortical and juxtamedullary nephrons. Furthermore, it also reports the expression of NaPi-IIc transcripts in S1 segments of both populations of nephrons, though in agreement with our data, its relative abundance is much lower than that of NaPi-IIa. More importantly, it also describes the presence of NaPi-IIb mRNA in the thin descending and ascending limbs of the loop of Henle as well as the TAL. This pattern of expression confirms our own findings and implies that, due to the anatomical differences between both populations, transcription of NaPi-IIb mRNAs is restricted to juxtamedullary nephrons, whereas no signal is detected in cortical nephrons [56]. Ransick *et al.* describe expression levels of NaPi-IIb even lower than those of NaPi-IIc. Surprisingly, a second transcriptome analysis of mouse kidney single cells published recently by Park *et al.* describes the presence of NaPi-IIa mRNA not only in proximal tubules but also in a large percentage of podocytes as well as of cells of the loop of Henle, distal tubules and principal and intercalated cells [51] (supplementary Fig. 4B), possibly reflecting contamination of cells from these segments with the highly abundant NaPi-IIa transcript during preparation of single cells. However, in agreement with Ransick's report and with the data presented here, Park *et al.* show that expression of NaPi-IIb mRNA takes place specifically in the loop of Henle, whereas the proximal tubule is reported as the segment with larger number of cells expressing NaPi-IIc transcripts [51]. Moreover, the percentage of cells found to be positive for NaPi-IIb and NaPi-IIc transcripts is far lower than those positive for NaPi-IIa.

Immunofluorescence analysis in mouse kidneys using antibodies against NaPi-IIa and NaPi-IIb corroborated their pattern of expression at the RNA level. For NaPi-IIa and NaPi-IIc our immunolocalization here is in agreement with previous publications demonstrating their overlapping localization in early parts of the proximal tubule, with higher expression in juxtamedullary nephrons in animals on a normal or low Pi diet [17,53]. Moreover, we could demonstrate that while NaPi-IIa and NaPi-IIc do not colocalize with uromodulin, a urinary glycoprotein produced by the TAL of the loop of Henle, NaPi-IIb antibodies stained a small number of tubules also positive for uromodulin. In addition to confirming the TAL localization of NaPi-IIb, the sparse RNA and immunofluorescence signal of the cotransporter in renal tissue probably explains the failure of the antibody to detect the protein on Western blots. Of note, the NaPi-IIb orthologue from zebrafish is expressed at the apical membrane of renal and intestinal epithelia [23]. Our immunolocalization data is in contrast to a previous report where intracellular expression of NaPi-IIb at the protein level was described in kidneys from rats fed standard Pi, whereas in rats fed on high Pi the transporter was detected intracellularly or bound to the basolateral membrane [68]. This discrepancy may be related to the use of different antibodies. The specificity of the antibody used in our work was previously confirmed by peptide protection [28] and

by the lack of cross-reaction in intestinal samples from knockout mice [26], and validated here as well (supplementary Fig. 1), whereas a commercial antibody was used in the mentioned rat study.

The presence of an active Pi transporter in nephron segments beyond proximal tubules was postulated decades ago. This hypothesis was based on micropuncture studies published by Amiel *et al.* in 1970 showing that the delivery of Pi to superficial distal tubules in rats is higher than the concentration in ureteral urine, suggesting reabsorption of Pi by distal segments of the nephron [1]. Furthermore, this study postulated that distal transport was active and inhibited by PTH. In 1997 Greger *et al.* also reported higher delivery of Pi to superficial distal tubules than urinary excretion of Pi, though the authors failed to detect ^{32}P reabsorption by the terminal segments of the rat nephron [24]. However, they could detect reabsorption of Pi in the loop of Henle of thyroparathyroidectomized (TPTX) rats, suggesting that the transporter was sensitive to PTH. Also using micropuncture techniques, Jaeger *et al.* reported in 1983 that intravenous administration of potassium to rats increases the Pi-reabsorbing capacity of the distal tubule, though they could not detect distal reabsorption in control rats [31]. However, in this study the effect of potassium was abrogated in thyro-parathyroidectomized animals suggesting a mechanism different from those described above. In contrast to these reports, other investigators failed to detect distal transport of Pi [11,67], attributing the previous observations to nephron heterogeneity, since proximal tubules of cortical nephrons (the ones accessible to micropuncture) reabsorb Pi less avidly than proximal tubules of juxtamedullary nephrons. Whether or not NaPi-IIb could be implicated in this putative distal transport remains to be investigated.

The mRNA expression of NaPi-IIb in kidney is not regulated neither by acute nor by chronic changes in dietary Pi. This is not surprising since most reports agree on the lack of effect of acute changes on dietary Pi on transcription of renal cotransporters [9,57,35], though there are contradictory reports regarding the effect of chronically provided diets [9,43]. Similarly, the renal abundance of NaPi-IIb transcripts is affected neither by the absence of NaPi-IIc in kidney nor by depletion of intestinal NaPi-IIb, showing just a minor increase in NaPi-IIa deficient mice. Instead, we found that NaPi-IIb mRNA expression is highly upregulated in kidneys of mice with oxalate nephropathy, in contrast to NaPi-IIa and NaPi-IIc, which are downregulated. Oxalate feeding has been shown as a model of crystal nephropathy leading to chronic kidney disease in mice [37,46,47]. In our hands, oxalate treatment resulted in kidney damage, as indicated by the reduced creatinine clearance and tendency for reduced urinary excretion of Pi. Furthermore, treated mice showed the expected increase of both plasma phosphate and FGF-23 production (plasma levels and renal mRNA expression), and showed signs of inflammation (high renal *Tnf* mRNA levels). Increased expression and activity of NaPi-IIb in the setting of chronic kidney disease might contribute to enhanced Pi reabsorption and maintenance of phosphate overload.

In summary, we have shown that kidneys from mice, rats and humans express NaPi-IIb mRNA at levels comparable to those of NaPi-IIc. In mice, renal NaPi-IIb colocalizes at the protein level with uromodulin, but not with NaPi-IIa or NaPi-IIc. The expression of NaPi-IIb transcripts in kidneys from mice is not regulated by dietary Pi and it is not altered in several Slc34 deficient models, except for a small upregulation in NaPi-IIa deficient mice. However, while NaPi-IIa and NaPi-IIc mRNAs are downregulated in a model of oxalate-induced kidney disease, the expression of NaPi-IIb transcripts is upregulated.

Figure legends

Figure 1. Renal mRNA expression of Na/Pi cotransporters in kidneys: real-time PCR. Relative mRNA expression of NaPi-IIa, NaPi-IIb, NaPi-IIc, Pit-1 and Pit-2 in kidneys of **A)** mice (n=5) and **B)** rats (n=5) fed on standard chow as well as in **C)** cortical sections of human kidneys (n=5). Ct values of each mRNA were normalized to the Ct values of HPRT.

Figure 2. Renal mRNA localization of Na/Pi cotransporters: *in situ* hybridization. **A)** Pattern of expression of NaPi-IIa (red) and NaPi-IIb (green) mRNAs in mouse kidney using fluorescently labelled *in situ* hybridization probes. Images on the left column show merged signals, whereas images on the middle and right columns show NaPi-IIa and NaPi-IIb mRNA signals individually. Images in the top row were taken in the renal cortex while the pictures in the middle and bottom rows were taken in medulla. **B)** Pattern of expression of NaPi-IIb in mouse kidney using a chromogenic *in situ* hybridization probe. White bars represent 25 μm.

Figure 3. Renal protein localization of Slc34 Na/Pi cotransporters. Kidney slices from mice were co-stained with antibodies against uromodulin together with antibodies against either **A)** NaPi-IIa, **B)** NaPi-IIb or **C)** NaPi-IIc. The uromodulin-related signal is shown in green and the cotransporters expression in red. White bars represent 25 μm.

Figure 4. Renal mRNA expression of Na/Pi cotransporters in wild type mice fed low or high Pi. Relative mRNA expression of NaPi-IIa, NaPi-IIb, NaPi-IIc and Pit-2 in kidneys of mice fed low (L) or high (H) Pi diets either **A)** acutely (18 hours; n=5) or **B)** chronically (5 days; n=5). Ct values of each mRNA were normalized to the Ct values of the control mRNA HPRT. * P< 0.05; unpaired t-test.

Figure 5. Renal mRNA expression of Na/Pi cotransporters in wild type and Slc34 depleted mice. Relative mRNA expression of NaPi-IIa, NaPi-IIb, NaPi-IIc, Pit-1 and Pit-2 in kidneys of mice deficient for **A)** NaPi-IIa (n= 4), **B)** intestinal NaPi-IIb (n=8) or **C)** renal NaPi-IIc (n=8) and their respective wild type littermates (sample size similar to the KO group). Ct values of each mRNA were normalized to the Ct values of the control mRNA HPRT. ** P< 0.001; **** P< 0.0001; unpaired t-test.

Figure 6. Effect of oxalate treatment of wild type mice. **A)** Creatinine clearance, **B)** urinary Pi, **C)** plasma Pi, **D)** plasma intact FGF-23, **E)** renal *Fgf23* mRNA **F)** renal *Tnf* mRNA in wild type mice treated with a control (white bars) or oxalate-rich (back bars) diet. **G)** Renal mRNA expression of Slc34 and Slc20 Na/Pi cotransporters. Ct values of tested genes were normalized to the Ct values of 18S mRNA. n=6 for both groups in all determinations. ** p<0.01, *** p< 0.001. Student t-test

Supplementary table 1 Sequence or source and efficiency of qPCR primers (Fw= forward; Rv= reverse) and probes used to quantify the expression of Slc20 and Slc34 cotransporters in samples from mice, rats and human.

Supplementary Figure 1. Validation of the anti NaPi-IIb antibody A-D) Immunofluorescence of mouse ileum with an anti-NaPi-IIb antibody (green) as well as with DAPI (blue) and phalloidin (red). **A, B)** signal in the absence of the antigenic peptide. **C, D)** signal in the presence of the antigenic peptide. **E-F)** Westernblots on kidney homogenates (K) and intestinal BBM (I) of mice using anti-NaPi-IIb (top panels) and actin (bottom panels) antibodies. Signals **E)** without or **F)** with antigenic peptide. The arrowhead indicates the position of the transporter in BBM isolated from ileum.

Figure 2. Intestinal mRNA expression of Na/Pi cotransporters: real-time PCR. Relative mRNA expression of NaPi-IIa, NaPi-IIb, NaPi-IIc, Pit-1 and Pit-2 in **A)** ileum of WT mice (n=5) as well as **B)** duodenum and **C)** jejunum from rats (n=5). Expression of Pit-1 in rat duodenum was not tested. Ct values of each mRNA were normalized to the Ct values of the control mRNA HPRT.

Supplementary Figure 3. Effect of oxalate treatment on wild type mice A) Plasma creatinine, and **B)** plasma urea. n=6. ** p<0.01, *** p< 0.001. Student t-test

Supplementary Figure 4. Data from single cell transcriptome analysis from mouse kidneys A) Expression of NaPi-IIa, NaPi-IIb and NaPi-IIc mRNAs in juxtamedullary nephrons and ureteric epithelium. Scheme taken from Ransick *et al*; Developmental Cell, 2019. Average expressions are given in logarithmic scale. Subdivisions indicate: **1)** podocytes (visceral epithelium), **2)** parietal epithelium, **3)** segment 1 of proximal tubule – female, **4)** segment 1 of proximal tubule – male, **5)** segment 2 of proximal tubule –female, **6)** segment 2 of proximal tubule – male, **7)** segment 3 of proximal tubule – female, **8)** segment 3 of proximal tubule – male, **9A)** LOH thin descending limb of inner stripe of outer medulla of cortical nephron, **9B)** LOH thin descending limb of inner stripe of outer medulla of juxtamedullary nephron, **10)** upper LOH thin descending limb of inner medulla of juxtamedullary nephron, **11)** lower LOH thin descending limb of inner medulla of juxtamedullary nephron, **12)** lower LOH thin limb of inner medulla of juxtamedullary nephron, **13)** lower LOH thin limb of inner medulla of juxtamedullary nephron, **14)** upper LOH thin ascending limb of inner medulla of juxtamedullary nephron, **15)** distal straight tubule of inner stripe of outer medulla (syn: thick ascending limb of LOH), **16)** distal straight tubule of outer stripe of outer medulla and cortex (syn: thick ascending limb of LOH), **17)** macula densa, **18)** distal convoluted tubule, **19)** nephron connecting tubule, **20)** principal-like cell of nephron connecting tubule, **21)** intercalated type non-A non-B cell of nephron connecting tubule, **22)** intercalated type A cell of nephron connecting tubule and cortical collecting duct, **23)** principal-like cell of cortical collecting duct, **24)** intercalated type B cell of cortical collecting duct, **25)** intercalated type A cell of outer medullary collecting duct, **26)** principal cell of outer medullary collecting duct, **27)** intercalated type A cell of inner medullary collecting duct, **28)** principal cell of inner medullary collecting duct type 1, **29)** principal cell of inner medullary collecting duct type 2, **30)** principal-like cell of deep inner medullary collecting duct type 1, **31)** cell of deep inner medullary collecting duct type 2

and **32)** deep medullary epithelium of pelvis. **B) Expression of NaPi-IIa, NaPi-IIb, NaPi-IIc, Pit-1 and Pit-2 mRNAs in kidneys from mice.** Data extracted from Park *et al*. Science 2018.

References

1. Amiel C, Kuntziger H, Richet G (1970) Micropuncture study of handling of phosphate by proximal and distal nephron in normal and parathyroidectomized rat. Evidence for distal reabsorption. Pflugers Arch 317:93-109. doi:10.1007/bf00592495
2. Bacic D, Capuano P, Baum M, Zhang J, Stange G, Biber J, Kaissling B, Moe OW, Wagner CA, Murer H (2005) Activation of dopamine D1-like receptors induces acute internalization of the renal Na+/phosphate cotransporter NaPi-IIa in mouse kidney and OK cells. Am J Physiol Renal Physiol 288:F740-747. doi:00380.2004 [pii]

10.1152/ajprenal.00380.2004
3. Beck L, Karaplis AC, Amizuka N, Hewson AS, Ozawa H, Tenenhouse HS (1998) Targeted inactivation of Npt2 in mice leads to severe renal phosphate wasting, hypercalciuria, and skeletal abnormalities. Proc Natl Acad Sci U S A 95:5372-5377. doi:10.1073/pnas.95.9.5372
4. Bergwitz C, Roslin NM, Tieder M, Loredo-Osti JC, Bastepe M, Abu-Zahra H, Frappier D, Burkett K, Carpenter TO, Anderson D, Garabedian M, Sermet I, Fujiwara TM, Morgan K, Tenenhouse HS, Juppner H (2006) SLC34A3 mutations in patients with hereditary hypophosphatemic rickets with hypercalciuria predict a key role for the sodium-phosphate cotransporter NaPi-IIc in maintaining phosphate homeostasis. Am J Hum Genet 78:179-192. doi:S0002-9297(07)62351-9 [pii]

10.1086/499409
5. Biber J, Hernando N, Forster I (2013) Phosphate transporters and their function. Annu Rev Physiol 75:535-550. doi:10.1146/annurev-physiol-030212-183748
6. Biber J, Stieger B, Stange G, Murer H (2007) Isolation of renal proximal tubular brush-border membranes. Nat Protoc 2:1356-1359. doi:10.1038/nprot.2007.156
7. Bon N, Couasnay G, Bourgine A, Sourice S, Beck-Cormier S, Guicheux J, Beck L (2018) Phosphate (Pi)-regulated heterodimerization of the high-affinity sodium-dependent Pi transporters PiT1/Slc20a1 and PiT2/Slc20a2 underlies extracellular Pi sensing independently of Pi uptake. J Biol Chem 293:2102-2114. doi:10.1074/jbc.M117.807339
8. Bon N, Frangi G, Sourice S, Guicheux J, Beck-Cormier S, Beck L (2018) Phosphate-dependent FGF23 secretion is modulated by PiT2/Slc20a2. Mol Metab 11:197-204. doi:10.1016/j.molmet.2018.02.007
9. Bourgeois S, Capuano P, Stange G, Muhlemann R, Murer H, Biber J, Wagner CA (2013) The phosphate transporter NaPi-IIa determines the rapid renal adaptation to dietary phosphate intake in mouse irrespective of persistently high FGF23 levels. Pflug Arch Eur J Phy 465:1557-1572. doi:10.1007/s00424-013-1298-9
10. Breusegem SY, Takahashi H, Giral-Arnal H, Wang X, Jiang T, Verlander JW, Wilson P, Miyazaki-Anzai S, Sutherland E, Caldas Y, Blaine JT, Segawa H, Miyamoto K, Barry NP, Levi M (2009) Differential regulation of the renal sodium-phosphate cotransporters NaPi-IIa, NaPi-IIc, and PiT-2 in dietary potassium deficiency. Am J Physiol Renal Physiol 297:F350-361. doi:90765.2008 [pii]

10.1152/ajprenal.90765.2008
11. Brunette MG, Taleb L, Carriere S (1973) Effect of parathyroid hormone on phosphate reabsorption along the nephron of the rat. Am J Physiol 225:1076-1081. doi:10.1152/ajplegacy.1973.225.5.1076
12. Candeal E, Caldas YA, Guillen N, Levi M, Sorribas V (2017) Intestinal phosphate absorption is mediated by multiple transport systems in rats. Am J Physiol-Gastr L 312:G355-G366. doi:10.1152/ajpgi.00244.2016
13. Capuano P, Radanovic T, Wagner CA, Bacic D, Kato S, Uchiyama Y, St-Arnoud R, Murer H, Biber J (2005) Intestinal and renal adaptation to a low-Pi diet of type II NaPi cotransporters in vitamin

D receptor- and 1alphaOHase-deficient mice. American journal of physiology Cell physiology 288:C429-434. doi:10.1152/ajpcell.00331.2004
14. Chen G, Liu Y, Goetz R, Fu L, Jayaraman S, Hu MC, Moe OW, Liang G, Li X, Mohammadi M (2018) alpha-Klotho is a non-enzymatic molecular scaffold for FGF23 hormone signalling. Nature 553:461-466. doi:10.1038/nature25451
15. Corut A, Senyigit A, Ugur SA, Altin S, Ozcelik U, Calisir H, Yildirim Z, Gocmen A, Tolun A (2006) Mutations in SLC34A2 cause pulmonary alveolar microlithiasis and are possibly associated with testicular microlithiasis. Am J Hum Genet 79:650-656. doi:S0002-9297(07)63075-4 [pii]

10.1086/508263
16. Cunningham R, Biswas R, Brazie M, Steplock D, Shenolikar S, Weinman EJ (2009) Signaling pathways utilized by PTH and dopamine to inhibit phosphate transport in mouse renal proximal tubule cells. Am J Physiol Renal Physiol 296:F355-361. doi:10.1152/ajprenal.90426.2008
17. Custer M, Lotscher M, Biber J, Murer H, Kaissling B (1994) Expression of Na-P-I Cotransport in Rat-Kidney - Localization by Rt-Pcr and Immunohistochemistry. Am J Physiol 266:F767-F774
18. Deliot N, Hernando N, Horst-Liu Z, Gisler SM, Capuano P, Wagner CA, Bacic D, O'Brien S, Biber J, Murer H (2005) Parathyroid hormone treatment induces dissociation of type IIa Na+-P(i) cotransporter-Na+/H+ exchanger regulatory factor-1 complexes. Am J Physiol Cell Physiol 289:C159-167. doi:00456.2004 [pii]

10.1152/ajpcell.00456.2004
19. Dinour D, Davidovits M, Ganon L, Ruminska J, Forster IC, Hernando N, Eyal E, Holtzman EJ, Wagner CA (2016) Loss of function of NaPiIIa causes nephrocalcinosis and possibly kidney insufficiency. Pediatr Nephrol. doi:10.1007/s00467-016-3443-0

10.1007/s00467-016-3443-0 [pii]
20. Forster IC, Hernando N, Biber J, Murer H (2012) Phosphate transport kinetics and structure-function relationships of SLC34 and SLC20 proteins. Curr Top Membr 70:313-356. doi:10.1016/B978-0-12-394316-3.00010-7
21. Forster IC, Hernando N, Biber J, Murer H (2013) Phosphate transporters of the SLC20 and SLC34 families. Mol Aspects Med 34:386-395. doi:S0098-2997(12)00090-8 [pii]

10.1016/j.mam.2012.07.007
22. Giral H, Caldas Y, Sutherland E, Wilson P, Breusegem S, Barry N, Blaine J, Jiang T, Wang XX, Levi M (2009) Regulation of rat intestinal Na-dependent phosphate transporters by dietary phosphate. Am J Physiol Renal Physiol 297:F1466-1475. doi:00279.2009 [pii]

10.1152/ajprenal.00279.2009
23. Graham C, Nalbant P, Scholermann B, Hentschel H, Kinne RK, Werner A (2003) Characterization of a type IIb sodium-phosphate cotransporter from zebrafish (Danio rerio) kidney. Am J Physiol Renal Physiol 284:F727-736. doi:10.1152/ajprenal.00356.2002
24. Greger R, Lang F, Marchand G, Knox FG (1977) Site of renal phosphate reabsorption. Micropuncture and microinfusion study. Pflugers Arch 369:111-118. doi:10.1007/bf00591566
25. Hattenhauer O, Traebert M, Murer H, Biber J (1999) Regulation of small intestinal Na-P(i) type IIb cotransporter by dietary phosphate intake. Am J Physiol 277:G756-762. doi:10.1152/ajpgi.1999.277.4.G756
26. Hernando N, Myakala K, Simona F, Knopfel T, Thomas L, Murer H, Wagner CA, Biber J (2015) Intestinal Depletion of NaPi-IIb/Slc34a2 in Mice: Renal and Hormonal Adaptation. J Bone Miner Res 30:1925-1937. doi:10.1002/jbmr.2523
27. Hernando N, Wagner CA (2018) Mechanisms and Regulation of Intestinal Phosphate Absorption. Compr Physiol 8:1065-1090. doi:10.1002/cphy.c170024
28. Hilfiker H, Hattenhauer O, Traebert M, Forster I, Murer H, Biber J (1998) Characterization of a murine type II sodium-phosphate cotransporter expressed in mammalian small intestine. Proc Natl Acad Sci U S A 95:14564-14569. doi:10.1073/pnas.95.24.14564

29. Ichikawa S, Sorenson AH, Imel EA, Friedman NE, Gertner JM, Econs MJ (2006) Intronic deletions in the SLC34A3 gene cause hereditary hypophosphatemic rickets with hypercalciuria. J Clin Endocrinol Metab 91:4022-4027. doi:jc.2005-2840 [pii]

10.1210/jc.2005-2840
30. Inden M, Iriyama M, Zennami M, Sekine SI, Hara A, Yamada M, Hozumi I (2016) The type III transporters (PiT-1 and PiT-2) are the major sodium-dependent phosphate transporters in the mice and human brains. Brain Res 1637:128-136. doi:10.1016/j.brainres.2016.02.032
31. Jaeger P, Bonjour JP, Karlmark B, Stanton B, Kirk RG, Duplinsky T, Giebisch G (1983) Influence of acute potassium loading on renal phosphate transport in the rat kidney. Am J Physiol 245:F601-605
32. Jensen N, Schroder HD, Hejbol EK, Fuchtbauer EM, de Oliveira JR, Pedersen L (2013) Loss of function of Slc20a2 associated with familial idiopathic Basal Ganglia calcification in humans causes brain calcifications in mice. J Mol Neurosci 51:994-999. doi:10.1007/s12031-013-0085-6
33. Juan D, Liptak P, Gray TK (1976) Absorption of inorganic phosphate in the human jejunum and its inhibition by salmon calcitonin. J Clin Endocrinol Metab 43:517-522. doi:10.1210/jcem-43-3-517
34. Katai K, Miyamoto K, Kishida S, Segawa H, Nii T, Tanaka H, Tani Y, Arai H, Tatsumi S, Morita K, Taketani Y, Takeda E (1999) Regulation of intestinal Na+-dependent phosphate co-transporters by a low-phosphate diet and 1,25-dihydroxyvitamin D3. Biochem J 343 Pt 3:705-712
35. Katai K, Segawa H, Haga H, Morita K, Arai H, Tatsumi S, Taketani Y, Miyamoto K, Hisano S, Fukui Y, Takeda E (1997) Acute regulation by dietary phosphate of the sodium-dependent phosphate transporter (NaP(i)-2) in rat kidney. J Biochem 121:50-55. doi:10.1093/oxfordjournals.jbchem.a021569
36. Keusch I, Traebert M, Lotscher M, Kaissling B, Murer H, Biber J (1998) Parathyroid hormone and dietary phosphate provoke a lysosomal routing of the proximal tubular Na/Pi-cotransporter type II. Kidney Int 54:1224-1232. doi:10.1046/j.1523-1755.1998.00115.x
37. Knauf F, Asplin JR, Granja I, Schmidt IM, Moeckel GW, David RJ, Flavell RA, Aronson PS (2013) NALP3-mediated inflammation is a principal cause of progressive renal failure in oxalate nephropathy. Kidney Int 84:895-901. doi:10.1038/ki.2013.207
38. Kurosu H, Ogawa Y, Miyoshi M, Yamamoto M, Nandi A, Rosenblatt KP, Baum MG, Schiavi S, Hu MC, Moe OW, Kuro-o M (2006) Regulation of fibroblast growth factor-23 signaling by klotho. J Biol Chem 281:6120-6123. doi:C500457200 [pii]

10.1074/jbc.C500457200
39. Lassiter WE, Colindres RE (1982) Phosphate reabsorption in the distal convoluted tubule. Adv Exp Med Biol 151:21-32. doi:10.1007/978-1-4684-4259-5_3
40. Lederer E, Wagner CA (2019) Clinical aspects of the phosphate transporters NaPi-IIa and NaPi-IIb: mutations and disease associations. Pflug Arch Eur J Phy 471:137-148. doi:10.1007/s00424-018-2246-5
41. Lorenz-Depiereux B, Benet-Pages A, Eckstein G, Tenenbaum-Rakover Y, Wagenstaller J, Tiosano D, Gershoni-Baruch R, Albers N, Lichtner P, Schnabel D, Hochberg Z, Strom TM (2006) Hereditary hypophosphatemic rickets with hypercalciuria is caused by mutations in the sodium-phosphate cotransporter gene SLC34A3. Am J Hum Genet 78:193-201. doi:10.1086/499410
42. Lotscher M, Kaissling B, Biber J, Murer H, Levi M (1997) Role of microtubules in the rapid regulation of renal phosphate transport in response to acute alterations in dietary phosphate content. J Clin Invest 99:1302-1312. doi:10.1172/JCI119289
43. Madjdpour C, Bacic D, Kaissling B, Murer H, Biber J (2004) Segment-specific expression of sodium-phosphate cotransporters NaPi-IIa and -IIc and interacting proteins in mouse renal proximal tubules. Pflugers Arch 448:402-410. doi:10.1007/s00424-004-1253-x
44. Marks J, Lee GJ, Nadaraja SP, Debnam ES, Unwin RJ (2015) Experimental and regional variations in Na+-dependent and Na+-independent phosphate transport along the rat small intestine and colon. Physiol Rep 3. doi:UNSP e12281

10.14814/phy2.12281
45. Marks J, Srai SK, Biber J, Murer H, Unwin RJ, Debnam ES (2006) Intestinal phosphate absorption and the effect of vitamin D: a comparison of rats with mice. Exp Physiol 91:531-537. doi:expphysiol.2005.032516 [pii]

10.1113/expphysiol.2005.032516
46. Mulay SR, Eberhard JN, Pfann V, Marschner JA, Darisipudi MN, Daniel C, Romoli S, Desai J, Grigorescu M, Kumar SV, Rathkolb B, Wolf E, de Angelis MH, Bauerle T, Dietel B, Wagner CA, Amann K, Eckardt KU, Aronson PS, Anders HJ, Knauf F (2016) Oxalate-induced chronic kidney disease with its uremic and cardiovascular complications in C57BL/6 mice. Am J Physiol-Renal 310:F785-F795. doi:10.1152/ajprenal.00488.2015
47. Mulay SR, Kulkarni OP, Rupanagudi KV, Migliorini A, Darisipudi MN, Vilaysane A, Muruve D, Shi Y, Munro F, Liapis H, Anders HJ (2013) Calcium oxalate crystals induce renal inflammation by NLRP3-mediated IL-1 beta secretion. J Clin Invest 123:236-246. doi:10.1172/Jci63679
48. Myakala K, Motta S, Murer H, Wagner CA, Koesters R, Biber J, Hernando N (2014) Renal-specific and inducible depletion of NaPi-IIc/Slc34a3, the cotransporter mutated in HHRH, does not affect phosphate or calcium homeostasis in mice. Am J Physiol Renal Physiol 306:F833-843. doi:ajprenal.00133.2013 [pii]

10.1152/ajprenal.00133.2013
49. Nishimura M, Naito S (2008) Tissue-specific mRNA expression profiles of human solute carrier transporter superfamilies. Drug Metab Pharmacokinet 23:22-44. doi:JST.JSTAGE/dmpk/23.22 [pii]
50. Nowik M, Picard N, Stange G, Capuano P, Tenenhouse HS, Biber J, Murer H, Wagner CA (2008) Renal phosphaturia during metabolic acidosis revisited: molecular mechanisms for decreased renal phosphate reabsorption. Pflug Arch Eur J Phy 457:539-549. doi:10.1007/s00424-008-0530-5
51. Park J, Shrestha R, Qiu C, Kondo A, Huang S, Werth M, Li M, Barasch J, Susztak K (2018) Single-cell transcriptomics of the mouse kidney reveals potential cellular targets of kidney disease. Science 360:758-763. doi:10.1126/science.aar2131
52. Pfister MF, Ruf I, Stange G, Ziegler U, Lederer E, Biber J, Murer H (1998) Parathyroid hormone leads to the lysosomal degradation of the renal type II Na/P-i cotransporter. P Natl Acad Sci USA 95:1909-1914. doi:DOI 10.1073/pnas.95.4.1909
53. Picard N, Capuano P, Stange G, Mihailova M, Kaissling B, Murer H, Biber J, Wagner CA (2010) Acute parathyroid hormone differentially regulates renal brush border membrane phosphate cotransporters. Pflug Arch Eur J Phy 460:677-687. doi:10.1007/s00424-010-0841-1
54. Radanovic T, Wagner CA, Murer H, Biber J (2005) Regulation of intestinal phosphate transport - I. Segmental expression and adaptation to low-P-i diet of the type IIb Na+-P-i cotransporter in mouse small intestine. Am J Physiol-Gastr L 288:G496-G500. doi:10.1152/ajpgi.00167.2004
55. Rajagopal A, Braslavsky D, Lu JT, Kleppe S, Clement F, Cassinelli H, Liu DS, Liern JM, Vallejo G, Bergada I, Gibbs RA, Campeau PM, Lee BH (2014) Exome sequencing identifies a novel homozygous mutation in the phosphate transporter SLC34A1 in hypophosphatemia and nephrocalcinosis. J Clin Endocrinol Metab 99:E2451-2456. doi:10.1210/jc.2014-1517
56. Ransick A, Lindstrom NO, Liu J, Zhu Q, Guo JJ, Alvarado GF, Kim AD, Black HG, Kim J, McMahon AP (2019) Single-Cell Profiling Reveals Sex, Lineage, and Regional Diversity in the Mouse Kidney. Dev Cell 51:399-413 e397. doi:10.1016/j.devcel.2019.10.005
57. Ritthaler T, Traebert M, Lotscher M, Biber J, Murer H, Kaissling B (1999) Effects of phosphate intake on distribution of type II Na/Pi cotransporter mRNA in rat kidney. Kidney Int 55:976-983. doi:10.1046/j.1523-1755.1999.055003976.x
58. Sabbagh Y, O'Brien SP, Song W, Boulanger JH, Stockmann A, Arbeeny C, Schiavi SC (2009) Intestinal npt2b plays a major role in phosphate absorption and homeostasis. J Am Soc Nephrol 20:2348-2358. doi:ASN.2009050559 [pii]

10.1681/ASN.2009050559

59. Saito A, Nikolaidis NM, Amlal H, Uehara Y, Gardner JC, LaSance K, Pitstick LB, Bridges JP, Wikenheiser-Brokamp KA, McGraw DW, Woods JC, Sabbagh Y, Schiavi SC, Altinisik G, Jakopovic M, Inoue Y, McCormack FX (2015) Modeling pulmonary alveolar microlithiasis by epithelial deletion of the Npt2b sodium phosphate cotransporter reveals putative biomarkers and strategies for treatment. Sci Transl Med 7:313ra181. doi:10.1126/scitranslmed.aac8577
60. Schlingmann KP, Ruminska J, Kaufmann M, Dursun I, Patti M, Kranz B, Pronicka E, Ciara E, Akcay T, Bulus D, Cornelissen EA, Gawlik A, Sikora P, Patzer L, Galiano M, Boyadzhiev V, Dumic M, Vivante A, Kleta R, Dekel B, Levtchenko E, Bindels RJ, Rust S, Forster IC, Hernando N, Jones G, Wagner CA, Konrad M (2016) Autosomal-Recessive Mutations in SLC34A1 Encoding Sodium-Phosphate Cotransporter 2A Cause Idiopathic Infantile Hypercalcemia. J Am Soc Nephrol 27:604-614. doi:10.1681/ASN.2014101025
61. Segawa H, Kaneko I, Takahashi A, Kuwahata M, Ito M, Ohkido I, Tatsumi S, Miyamoto K (2002) Growth-related renal type II Na/Pi cotransporter. J Biol Chem 277:19665-19672. doi:10.1074/jbc.M200943200

M200943200 [pii]
62. Segawa H, Kaneko I, Yamanaka S, Ito M, Kuwahata M, Inoue Y, Kato S, Miyamoto K (2004) Intestinal Na-P(i) cotransporter adaptation to dietary P(i) content in vitamin D receptor null mice. Am J Physiol Renal Physiol 287:F39-47. doi:10.1152/ajprenal.00375.2003

00375.2003 [pii]
63. Segawa H, Kawakami E, Kaneko I, Kuwahata M, Ito M, Kusano K, Saito H, Fukushima N, Miyamoto K (2003) Effect of hydrolysis-resistant FGF23-R179Q on dietary phosphate regulation of the renal type-II Na/Pi transporter. Pflugers Arch 446:585-592. doi:10.1007/s00424-003-1084-1
64. Segawa H, Onitsuka A, Kuwahata M, Hanabusa E, Furutani J, Kaneko I, Tomoe Y, Aranami F, Matsumoto N, Ito M, Matsumoto M, Li M, Amizuka N, Miyamoto K (2009) Type IIc sodium-dependent phosphate transporter regulates calcium metabolism. J Am Soc Nephrol 20:104-113. doi:ASN.2008020177 [pii]

10.1681/ASN.2008020177
65. Segawa H, Yamanaka S, Onitsuka A, Tomoe Y, Kuwahata M, Ito M, Taketani Y, Miyamoto K (2007) Parathyroid hormone-dependent endocytosis of renal type IIc Na-Pi cotransporter. Am J Physiol Renal Physiol 292:F395-403. doi:00100.2006 [pii]

10.1152/ajprenal.00100.2006
66. Shimada T, Hasegawa H, Yamazaki Y, Muto T, Hino R, Takeuchi Y, Fujita T, Nakahara K, Fukumoto S, Yamashita T (2004) FGF-23 is a potent regulator of vitamin D metabolism and phosphate homeostasis. J Bone Miner Res 19:429-435. doi:10.1359/JBMR.0301264
67. Staum BB, Hamburger RJ, Goldberg M (1972) Tracer microinjection study of renal tubular phosphate reabsorption in the rat. J Clin Invest 51:2271-2276. doi:10.1172/JCI107036
68. Suyama T, Okada S, Ishijima T, Iida K, Abe K, Nakai Y (2012) High phosphorus diet-induced changes in NaPi-IIb phosphate transporter expression in the rat kidney: DNA microarray analysis. PLoS One 7:e29483. doi:10.1371/journal.pone.0029483

PONE-D-11-18908 [pii]
69. Tachibana T, Hagiwara K, Johkoh T (2009) Pulmonary alveolar microlithiasis: review and management. Curr Opin Pulm Med 15:486-490. doi:10.1097/MCP.0b013e32832d03bb
70. Tomoe Y, Segawa H, Shiozawa K, Kaneko I, Tominaga R, Hanabusa E, Aranami F, Furutani J, Kuwahara S, Tatsumi S, Matsumoto M, Ito M, Miyamoto K (2010) Phosphaturic action of fibroblast growth factor 23 in Npt2 null mice. Am J Physiol Renal Physiol 298:F1341-1350. doi:ajprenal.00375.2009 [pii]

10.1152/ajprenal.00375.2009
71. Villa-Bellosta R, Ravera S, Sorribas V, Stange G, Levi M, Murer H, Biber J, Forster IC (2009) The Na+-Pi cotransporter PiT-2 (SLC20A2) is expressed in the apical membrane of rat renal proximal

tubules and regulated by dietary Pi. Am J Physiol Renal Physiol 296:F691-699. doi:90623.2008 [pii]

10.1152/ajprenal.90623.2008

72. Wagner CA, Hernando N, Forster IC, Biber J (2014) The SLC34 family of sodium-dependent phosphate transporters. Pflugers Arch 466:139-153. doi:10.1007/s00424-013-1418-6
73. Wagner CA, Rubio-Aliaga I, Hernando N (2019) Renal phosphate handling and inherited disorders of phosphate reabsorption: an update. Pediatr Nephrol 34:549-559. doi:10.1007/s00467-017-3873-3
74. Walton J, Gray TK (1979) Absorption of Inorganic-Phosphate in the Human Small-Intestine. Clin Sci 56:407-412. doi:DOI 10.1042/cs0560407
75. Wang C, Li Y, Shi L, Ren J, Patti M, Wang T, de Oliveira JR, Sobrido MJ, Quintans B, Baquero M, Cui X, Zhang XY, Wang L, Xu H, Wang J, Yao J, Dai X, Liu J, Zhang L, Ma H, Gao Y, Ma X, Feng S, Liu M, Wang QK, Forster IC, Zhang X, Liu JY (2012) Mutations in SLC20A2 link familial idiopathic basal ganglia calcification with phosphate homeostasis. Nat Genet 44:254-256. doi:10.1038/ng.1077
76. Xu H, Bai L, Collins JF, Ghishan FK (2002) Age-dependent regulation of rat intestinal type IIb sodium-phosphate cotransporter by 1,25-(OH)(2) vitamin D(3). Am J Physiol Cell Physiol 282:C487-493. doi:10.1152/ajpcell.00412.2001

Figure 1

A) Mouse kidney

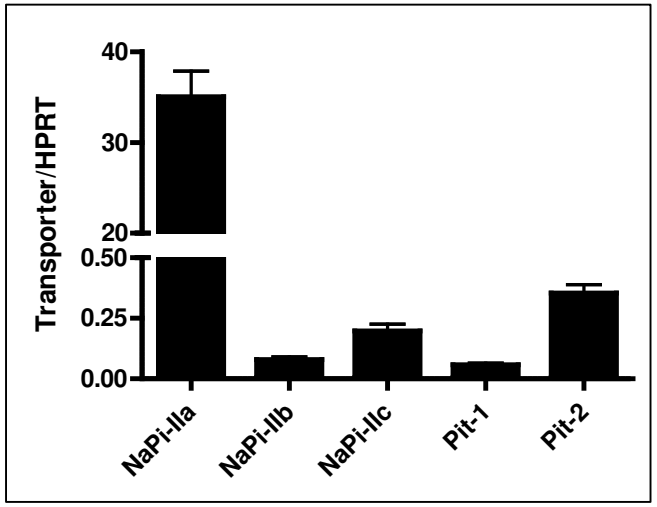

B) Rat kidney

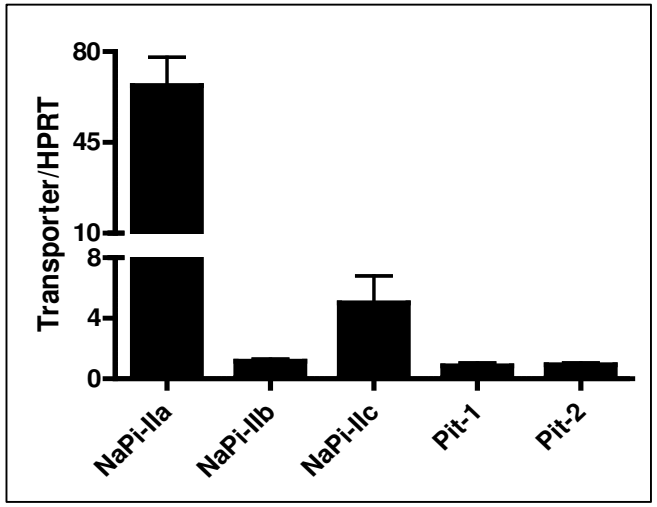

C) Human kidney

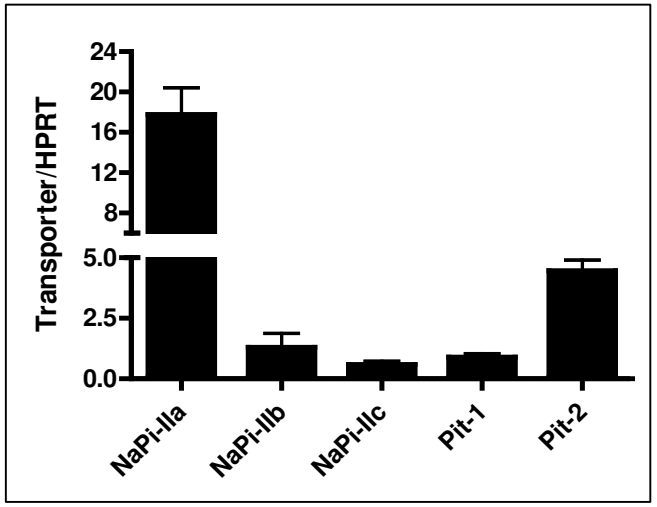

Figure 2

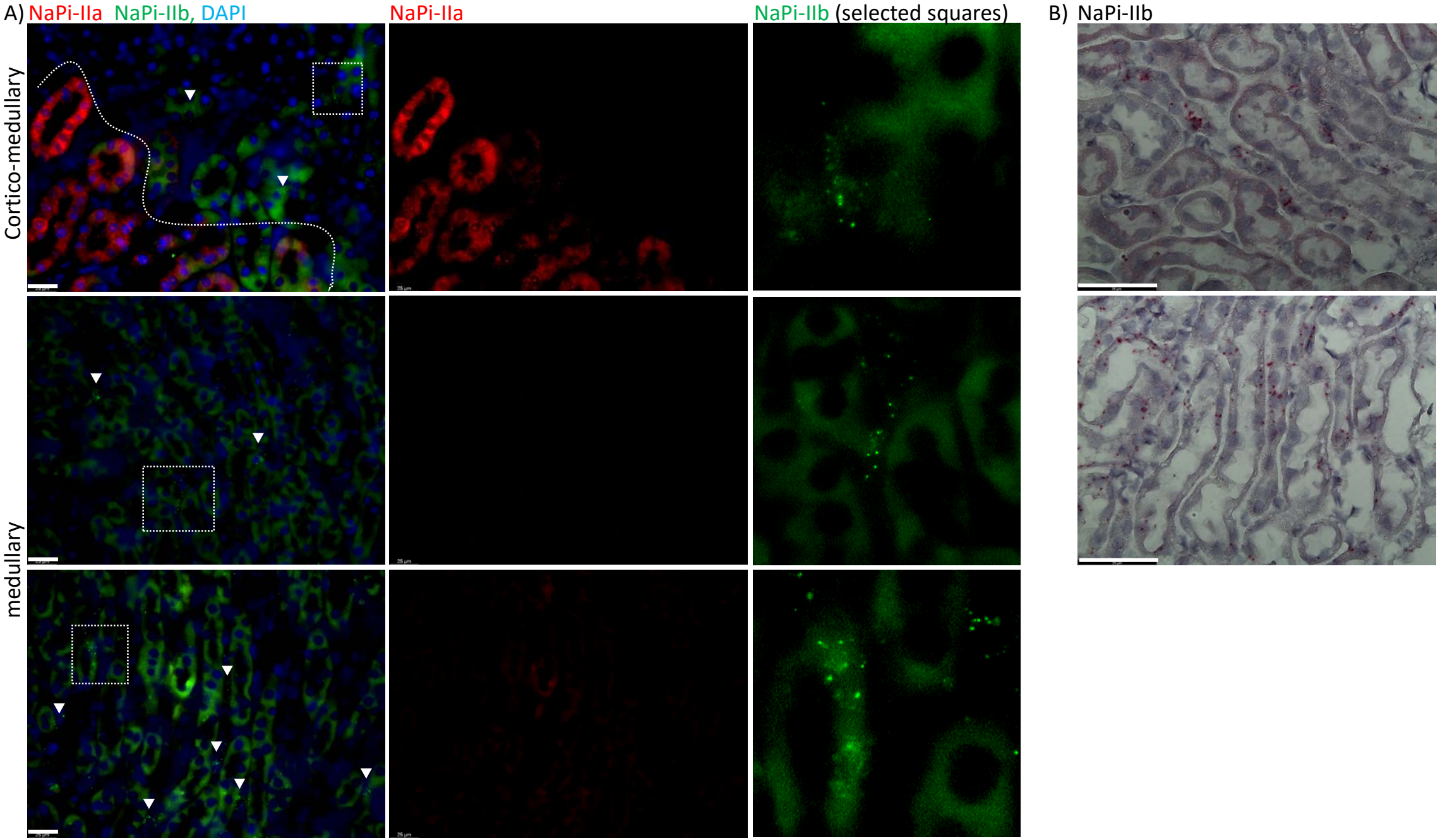
A) NaPi-IIa NaPi-IIb, DAPI
NaPi-IIa
NaPi-IIb (selected squares)
B) NaPi-IIb
Cortico-medullary
medullary

Figure 3

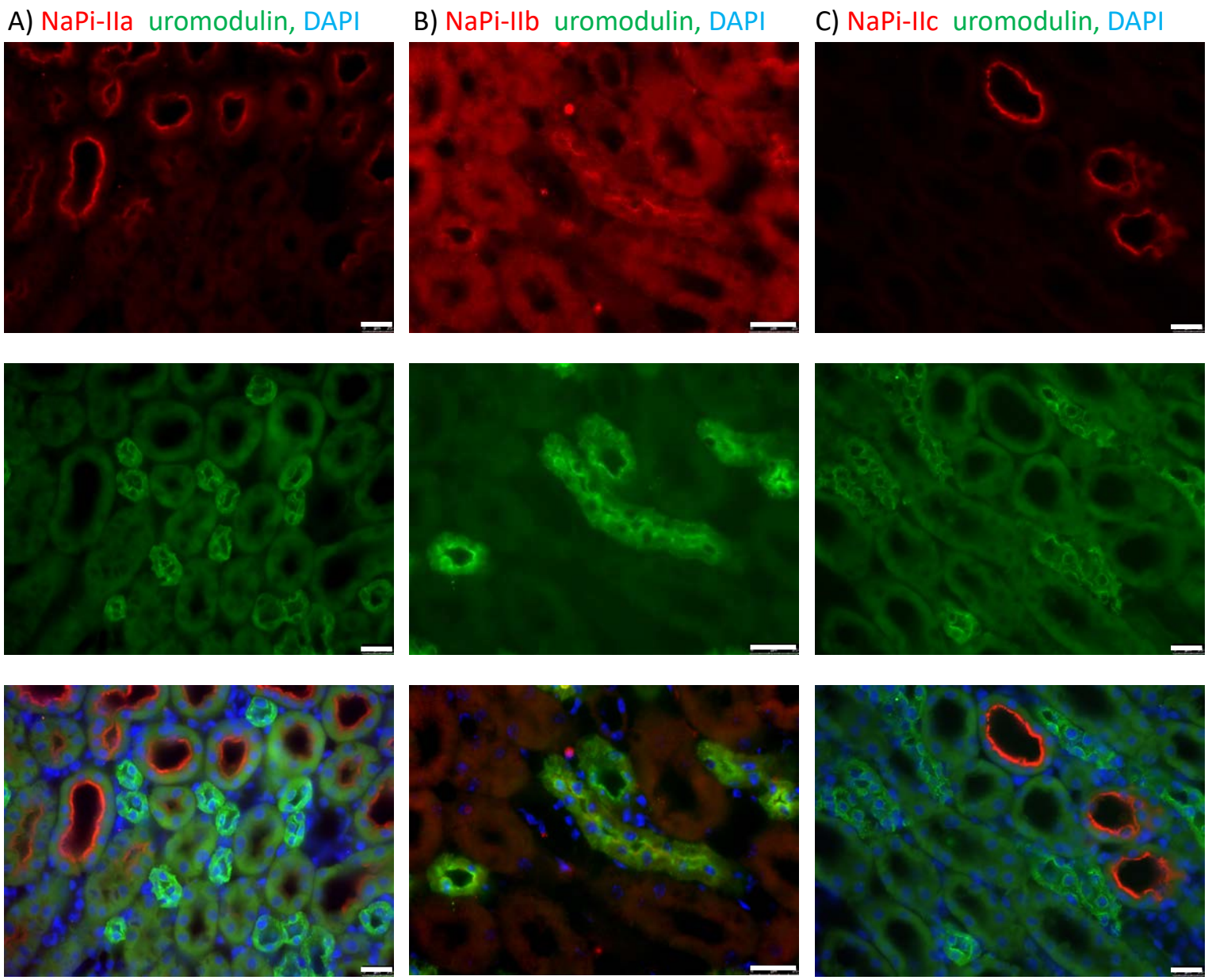
A) NaPi-IIa uromodulin, DAPI
B) NaPi-IIb uromodulin, DAPI
C) NaPi-IIc uromodulin, DAPI

Figure 4

A) Kidneys from WT mice fed 18 h H/L Pi

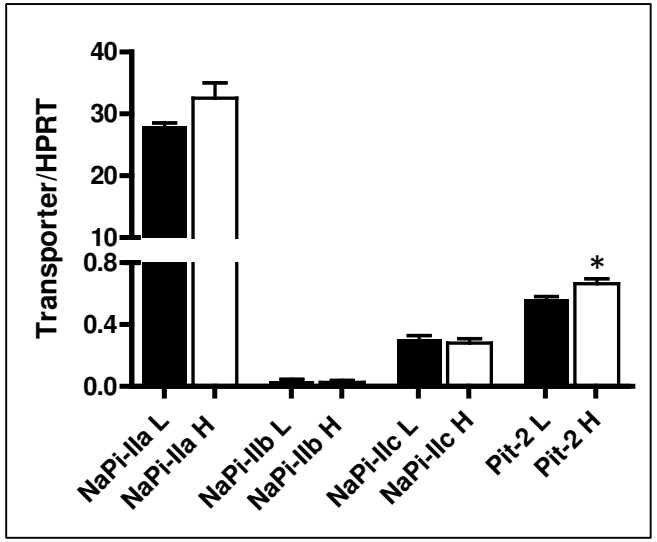

B) Kidneys from WT mice fed 5 days H/L Pi

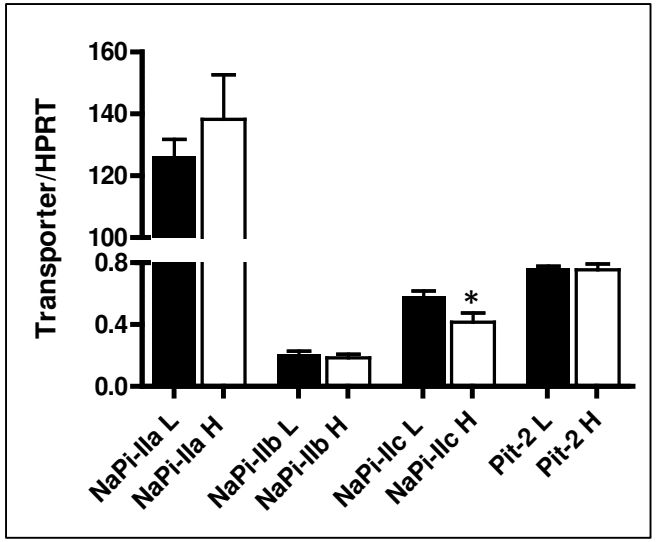

Figure 5

A) Kidneys from WT and global NaPi-IIa KOs

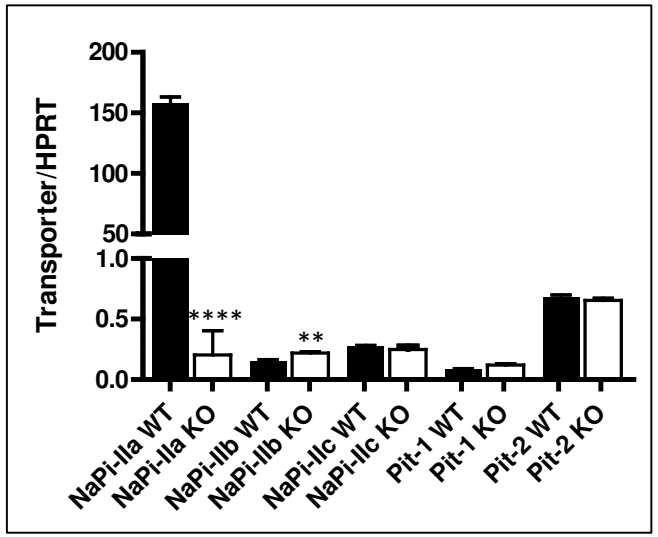

B) Kidneys from WT and intestinal-specific NaPi-IIb KOs

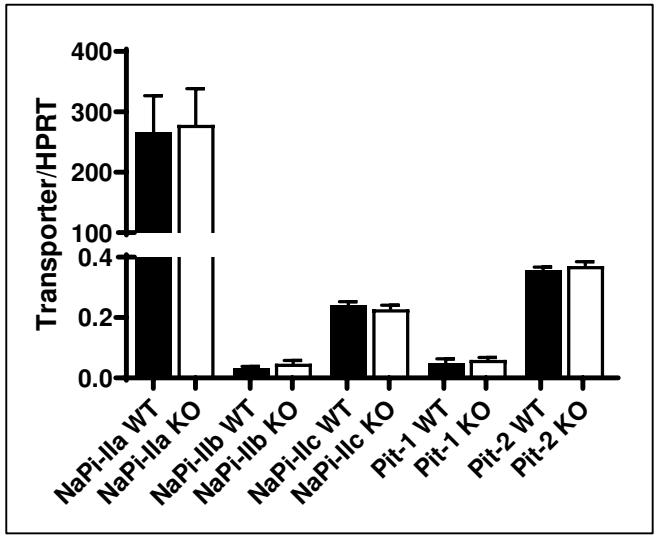

C) Kidneys from WT and renal-specific NaPi-IIc KOs

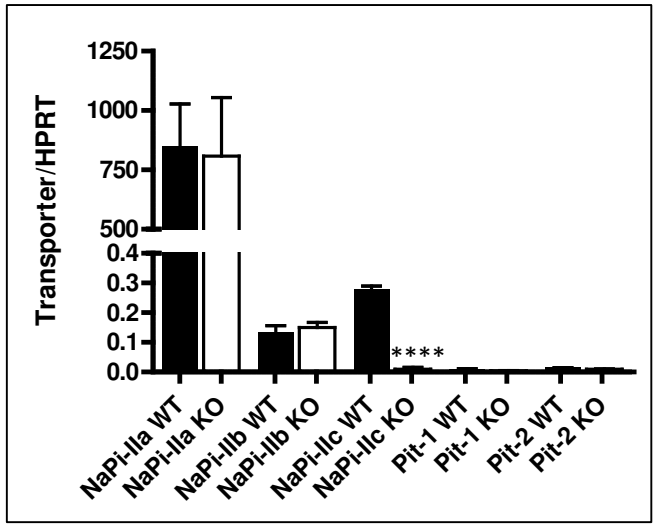

Figure 6

A) Creatinine clearance

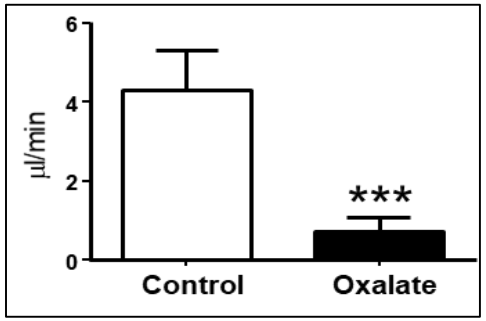

B) Urinary Pi

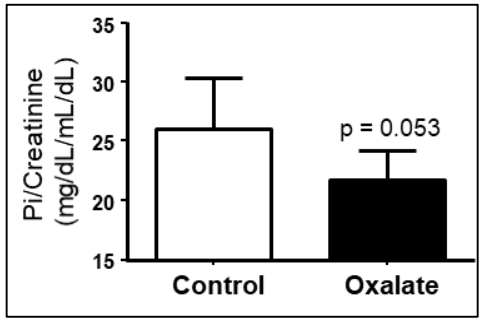

C) Plasma Pi

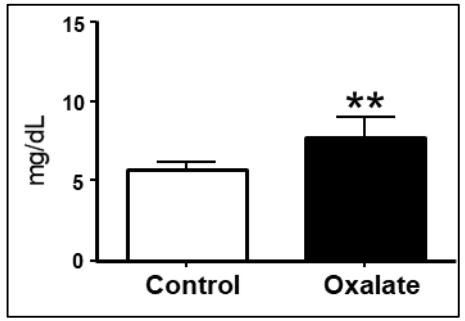

D) Plasma FGF-23

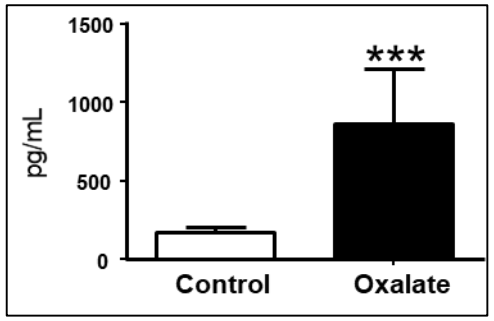

E) Fgf-23 mRNA

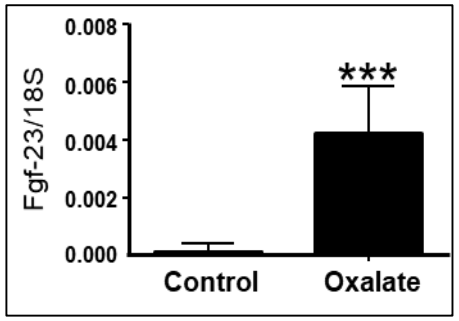

F) Tnf mRNA

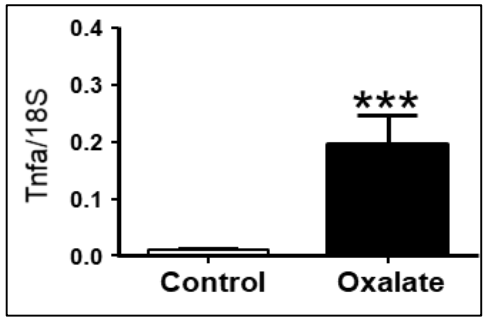

G) Renal expression of Na/Pi-cotransporters

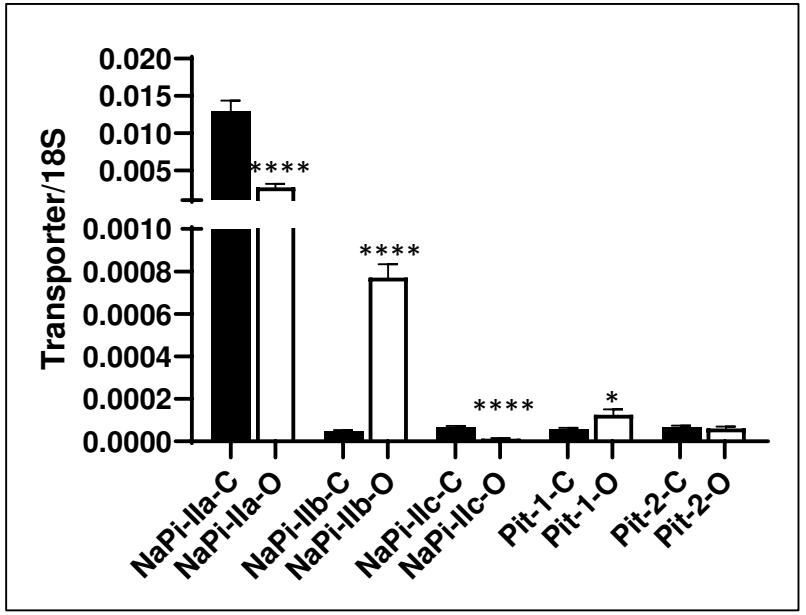

Supplementary table 1: sequences of primers and probes

Gene	Primer	Sequence	Efficiency
m-NaPi-IIa	Fw	TGATCACCAGCATTGCCG	
	Rv	GTGTTTGCAAGGCTGCCG	2.0
	Probe	CCAGACACAACAGAGGCTTCCACTTCTATGTC	
m-NaPi-IIb	Fw	CTTGGGACCTGCCTGAAC	
	Rv	AATGCAGAGCGTCTTCCCTTT	2.0
	Probe	TGGTCAGAGAGAGACAC	
m-NaPi-IIc	Fw	CAGCGGTATTACCAGCAACA	2.0
	Rv	CTGTCCTCCTCTGGAGATGC	
	Probe	GTGGCCTCTTCAGCTCTTGCACAGA	
m-Pit-1	Fw	CGCTGCTTTCTGGTATTATGTCTG	
	Rv	AGAGGTTGATTCCGATTGTGCA	1.9
	Probe	TTGTTCGTGCGTTCATCCTCCGTAAGG	
m-Pit-2	Fw	AGGAGTGCAGTGGATGGAGC	
	Rv	ATTAGTATGAACAGCACGCCGG	1.9
	Probe	ATTGTCGCCTCCTGGTTTATATCGCCAC	
m-HPRT	Fw	TTATCAGACTGAAGAGCTACTGTAATGATC	
	Rv	TTACCAGTGTCAATTATATCTTCAACAATC	1.9
	Probe	TGAGAGATCATCTCCACCAATAACTTTTATGTC	
r-NaPi-IIa	Fw	GGAATCACAGTCTCATTCGGATT	
	Rv	ATGGCCTCTACCCTGGACATAG	1.9
	Probe	TGTCAACCAGAGACAAAAGAGGCTTCCACT	
r-NaPi-IIb	Fw	TCAGGTCCACAGTCTAGCATACCA	
	Rv	CGGAATATGAGGGTAGAAGTTCAATC	1.8
	Probe	ACCAGCAAAACAAATGACAGCGGGAC	
r-NaPi-IIc	Fw	GCCTCTAAGTTGCTGACTGT	
	Rv	AGGCCCTCTGAAATTCATCC	1.9
	Probe	CACTCTGGTCTCGATGGCACAGTCA	
r-Pit-1	Fw	CCTGCTTTGGGTCCTTTGC	
	Rv	CAGCCACAGGGCCACAAG	1.9
	Probe	TGGCCTTCCCATCAGCACAACACATT	
r-Pit-2	Fw	CCTGCTTTGGGTCCTTTGC	
	Rv	CAGCCACAGGGCCACAAG	1.9
	Probe	ACGGTGGCAACGATGTGAGCAATG	
r-HPRT	Fw	GCTGAAGATTTGGAAAAGGTGTTA	
	Rv	ACACAGAGGGCCACAATGTGA	1.8
	Probe	TTATGGACAGGACTGAAAGACTTGCTCGAGATG	
h-NaPi-IIa		Applied Biosystem	2.0
h-NaPi-IIb	Fw	CCCAGATTAACGTCACTGTTC	
	Rv	CAAAGATATGCTGGCATTTGG	1.9
	Probe	AACTGCACCTCCCCTTCCCTCTGTT	
h-NaPi-IIc	Fw	GATGAATTTCAGAGGGCTTTCAG	
	Rv	GCTAGCTCACTTAGCCTCTC	1.9
	Probe	TGCACGGGATCTTCAACTGGCTCAC	
h-Pit-1	Fw	ATCCTCCATAAGGCAGATCC	
	Rv	ACATCCCACCGAGATGAG	1.8
	Probe	ACTGGAGCACCGTTGCTGGGCTTTG	
h-Pit-2		Applied Biosystem	2.0
h-HPRT	Fw	AAGGGTGTTTATTCCTCATGGACTA	
	Rv	GGCCTCCCATCTCCTTCATC	1.8
	Probe	TTATGGACAGGACTGAACGTCTTGC	

Supplementary figure 1

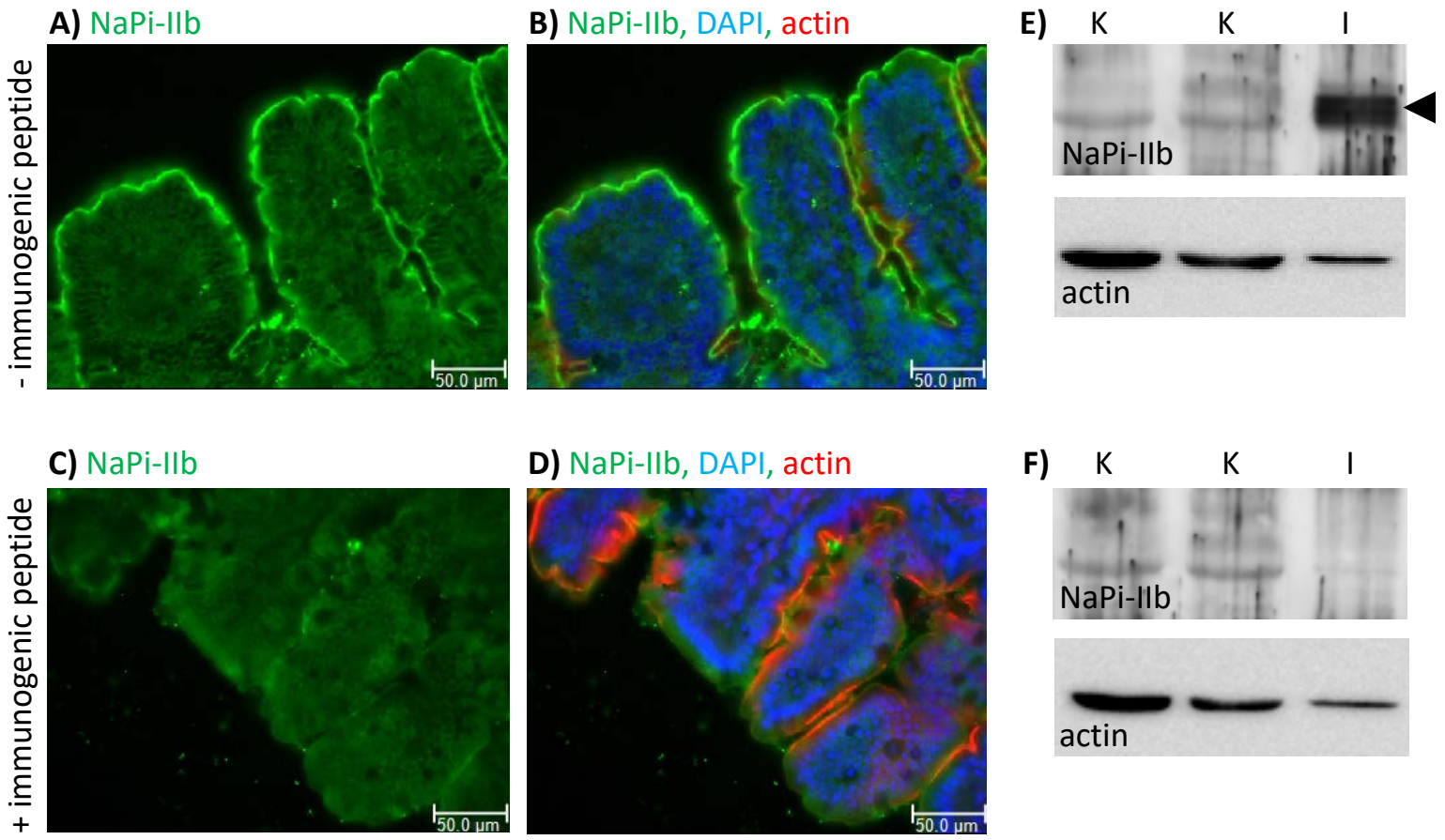

Supplementary figure 2

A) Mouse ileum

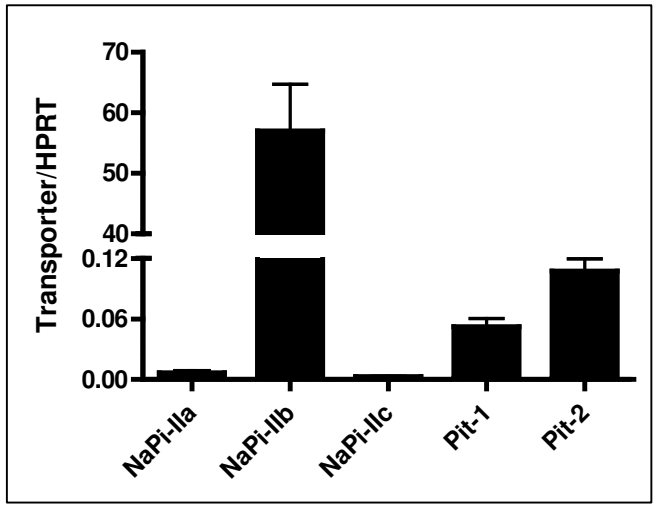

B) Rat duodenum

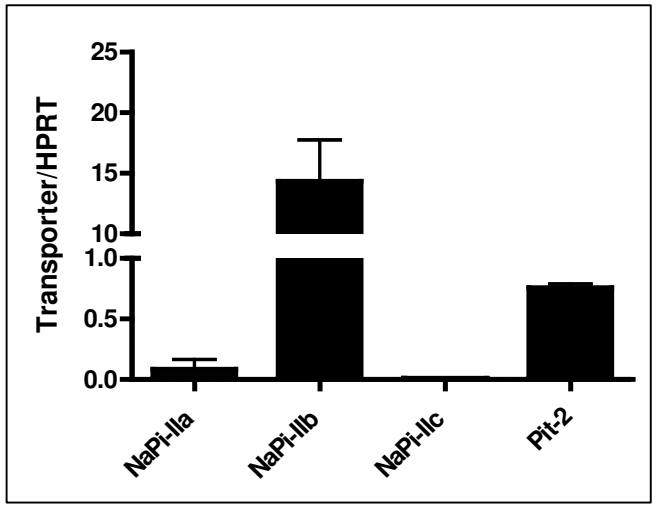

C) Rat jejunum

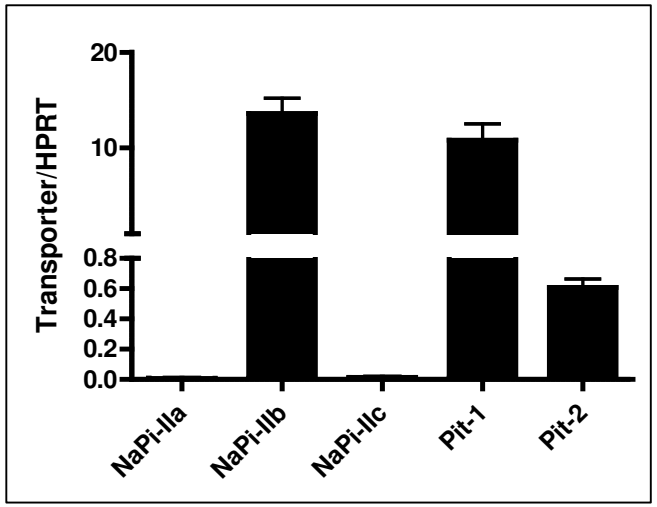

Supplemetary figure 3

A) Plasma creatinine

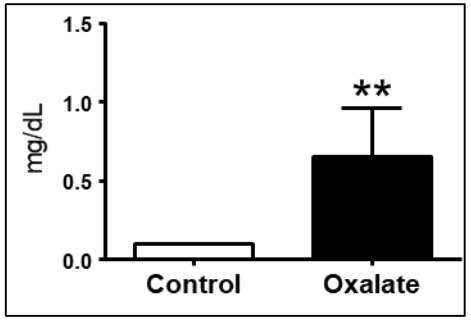

B) Plasma urea

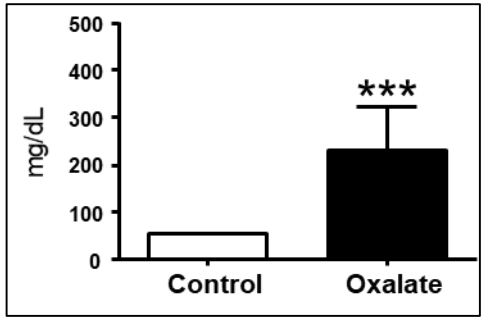

Supplementary Figure 4a

A) Ransick *et al*, 2019

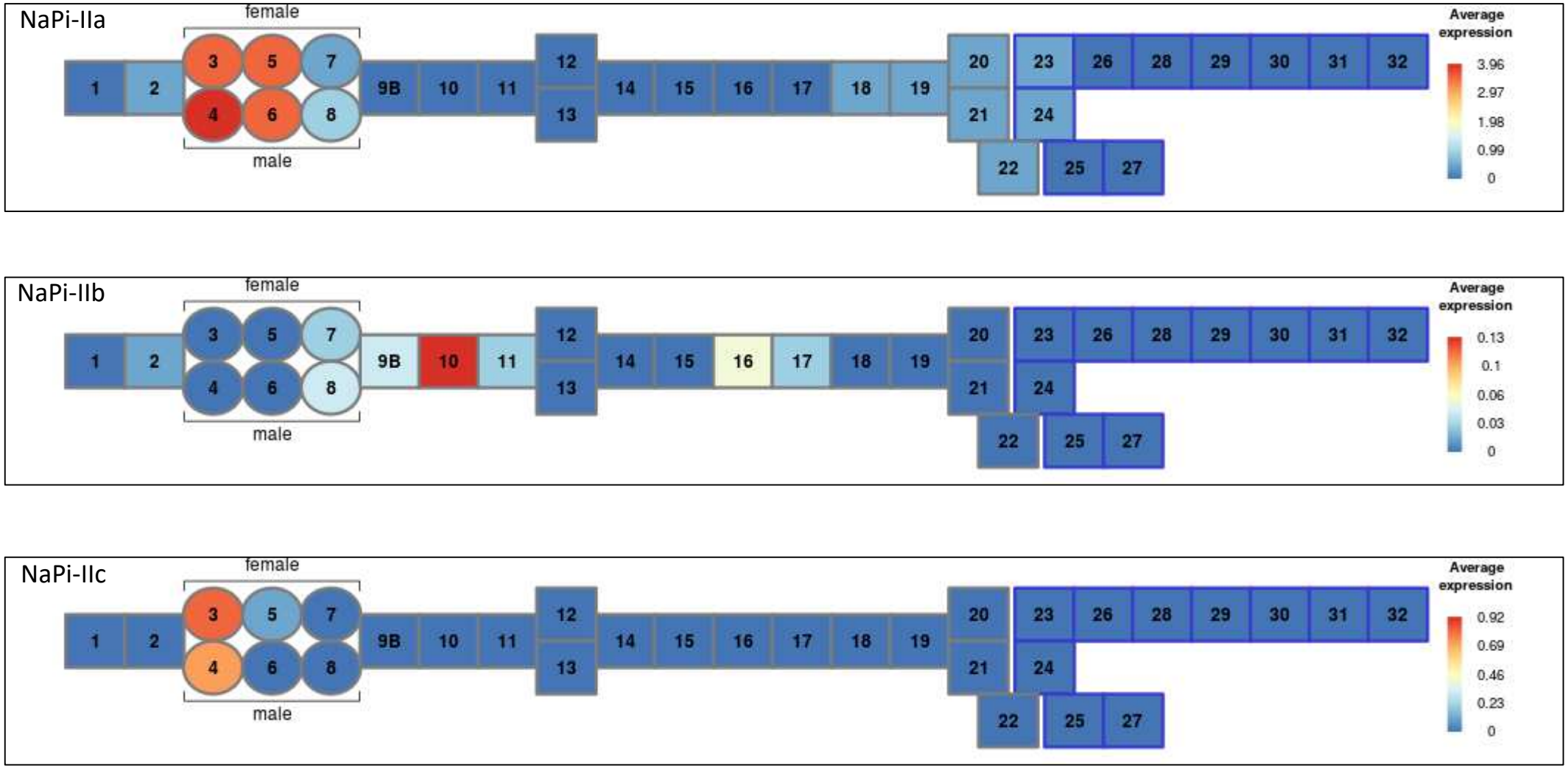

B) Park *et al*, 2018

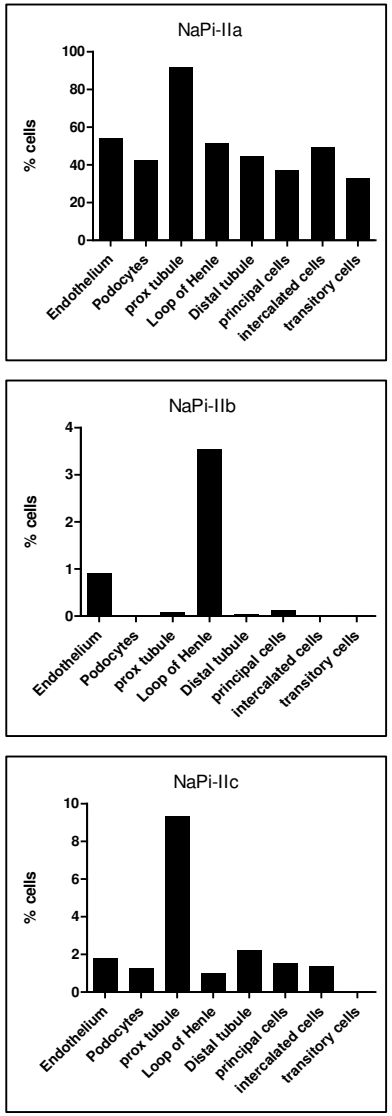

Supplementary Figure 4b

A) Ransick *et al*, 2019

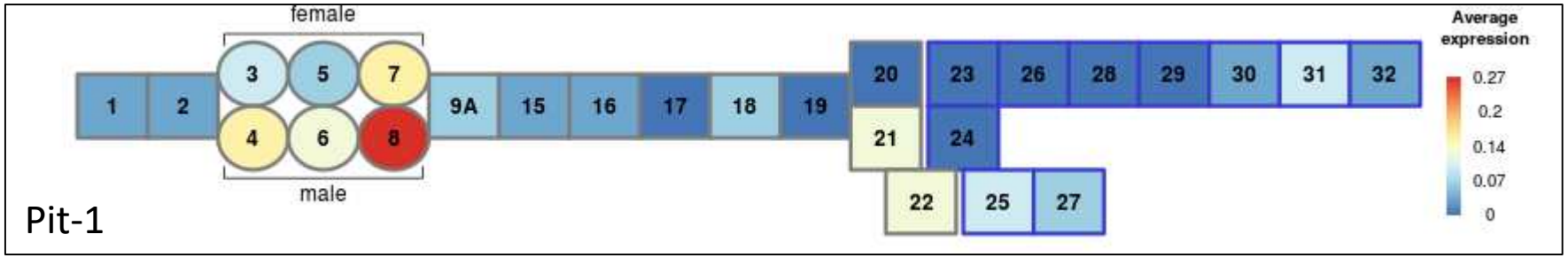

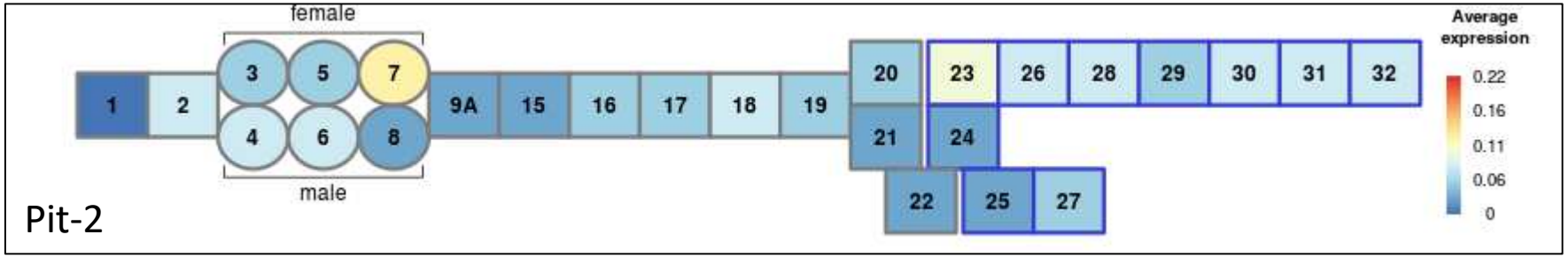

B) Park *et al*, 2018